



FUGRO CONSULTANTS, INC.

2012 Onshore Seismic Survey Report

PR No.: PGEQ-PR-21

Revision: 0

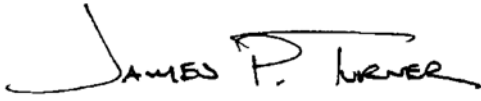
Page 1 of 81

PROJECT REPORT TITLE: PGEQ-PR-21
2012 3D Onshore Seismic Survey Report


PROJECT NAME: PG&E CCCSIP

PROJECT NO. 04.79225400 Phase 3 (FCL)

PPD NO: PGEQ-PPD-001

Prepared By: 
Date: 6/6/14

Jamey Turner, P.G.
Senior Geologist

Checked By: 
Date: 6/6/14

Dr. Daniel O'Connell
Senior Principal Geophysicist

Approved By: 
Date: 6/6/14

William Godwin, CEG
Principal Geologist



Project Report Revision Status			
Rev. No.	Date	Description	Impacted Document No.
0	6/6/14	Initial Issue	None
Text Revision History			
<u>Page No.</u>	<u>Rev. No.</u>	<u>Page No.</u>	<u>Rev. No.</u>
Attachment Revision History			
Attachment No.	Page No.	Rev. No.	Description



Item	Parameter	Yes	No	N/A
1	Purpose is clearly stated and Report satisfies the Purpose.	✓		
2	Methodology is appropriate and properly applied.	✓		
3	Assumptions are reasonable, adequately described, and based upon sound geotechnical principles and practices.	✓		
4	Input was authorized and correctly incorporated into the Report.	✓		
5	Software is properly identified and applied; and validation is referenced, or included, and acceptable.	✓		
6	Detailed Discussion is complete, accurate, and leads logical to Results and Conclusions.	✓		
7	Results and Conclusions are accurate, acceptable, and reasonable compared to the Input and Assumptions.	✓		
8	If commercial software, such as EXCEL, MATLAB, IDL, or Mathcad, was used, equations and other entries have been checked as necessary to ensure correct results.	✓		
9	References are valid for intended use.	✓		
10	Appendices are complete, accurate, and support text.	✓		

Comments: (use additional pages as necessary)


Verifier:  Date: 6/6/14
Daniel O'Connell, Senior Principal Geophysicist

TABLE OF CONTENTS

	Page
Signatories	1
Record of Revisions	2
Verification Summary	3
Lists of Tables, Figures, and Appendices	7
Abbreviations and Acronyms	11
1.0 INTRODUCTION	13
1.1 Background.....	15
1.2 Objectives and Approach	17
1.2.1 Phase 1 Objectives and Approach.....	17
1.2.2 Phase 2 Objectives and Approach.....	17
1.3 Quality Assurance.....	18
1.3.1 NQA-1 Program.....	19
1.3.2 Scope of Work.....	19
1.3.3 Safety-Related Software.....	20
2.0 ONSHORE 2012 3D DATA ACQUISITION.....	21
2.1 Phase 1 Data Acquisition	21
2.2 Phase 2 Data Acquisition	22
2.3 Resolution and Limitations of the Seismic Survey Data.....	23
2.3.1 Phase 1 DCPD 3D Data Acquisition Impacts.....	24
2.3.2 Phase 1 DCPD 3D Data Processing and Outputs for Interpretation ..	25
2.3.3 Phase 2 Marine Terrace 3D Impacts of Data Acquisition and Processing.....	27
2.3.4 3D Seismic-Reflection Resolution and Depth Extent.....	28
2.3.4.1 Phase 1 Seismic-Reflection Resolution and Depth Extent	28
2.3.4.2 Phase 2 Seismic-Reflection Resolution and Depth Extent	29

2.3.5	Constraints on Seismic Stratigraphy	31
2.3.6	Seismic-Reflection Data Image Acoustic Impedance Contrasts	31
2.3.7	3D Migration Isotropic Velocity Models	32
3.0	GEOLOGIC AND TECTONIC SETTING	36
3.1	Irish Hills Geology	36
3.1.1	Tectonic Setting	36
3.1.2	Geologic History	37
3.1.3	Irish Hills Gravity and Magnetic Structure	39
3.2	Phase 1 Geology	40
3.2.1	Phase 1 Geologic Mapping at the DCPD	40
3.2.2	Phase 1 Stratigraphy	40
3.2.3	Phase 1 Structure	41
3.3	Phase 2 Geology	42
3.3.1	Phase 2 Geologic Mapping	42
3.3.2	Phase 2 Stratigraphy	42
3.3.3	Phase 2 Structure	43
4.0	ANALYSIS, INTERPRETATION, AND RESULTS	47
4.1	Phase 1 Analysis, Interpretation, and Results	47
4.1.1	Phase 1 Methods of Analysis	47
4.1.2	Phase 1 Vp 3D Tomography Volume	48
4.1.3	Phase 1 Potential Field Magnetic and Gravity Data	51
4.1.3.1	Magnetic Data	51
4.1.3.2	Gravity	53
4.1.4	Phase 1 Isosurfaces	54
4.1.5	Phase 1 Seismic Reflection	55
4.1.5.1	Extracted Phase 1 SigSeis Seismic-Reflection Data	55
4.1.5.2	Phase 1 Seismic-Reflection Interpretation Criteria	55
4.1.5.3	Phase 1 2D SigSeis Reflection Profiles	57

4.1.5.4	2D SigSeis Reflection Vp Tomography Overlay Profiles.....	59
4.1.5.5	Phase 1 Seismic Horizon Mapping Framework and Uncertainties.....	60
4.1.6	Assessment of Mapped Structures near the DCPD	60
4.2	Phase 2 Analysis, Interpretation, and Results	63
4.2.1	Phase 2 Methods of Analysis.....	63
4.2.1.1	Phase 2 Vp Tomography Methods.....	63
4.2.1.2	Phase 2 Seismic-Reflection Data Methods	64
4.2.1.3	Phase 2 Methods Using Existing Geologic and Geophysical Data.....	66
4.2.2	Phase 2 Tomography Volume and Horizons.....	67
4.2.3	Phase 2 Seismic Reflection	69
4.2.3.1	Seismic-Reflector Discontinuity Mapping	70
4.2.4	Phase 2 Topographic Lineaments	72
4.2.5	Phase 2 Potential Field Magnetic Data	72
4.2.6	Assessment of Structures in the Phase 2 Area.....	73
4.2.6.1	Assessment of the Rattlesnake Fault.....	73
4.2.6.2	Assessment of Previously Unrecognized Structures	75
5.0	SUMMARY AND CONCLUSIONS.....	76
6.0	RECOMMENDATIONS.....	78
7.0	REFERENCES	79

	FUGRO CONSULTANTS, INC <i>2012 Onshore Seismic Survey Report</i>	PR No.: PGEQ-PR-21
		Revision: 0
		Page 7 of 81

LISTS OF TABLES, FIGURES, AND APPENDICES

Tables

Table 2-1	Summary of Seismic Survey Data
Table 3-1	Phase 2 Borehole Data Correlating Top-of-Rock Elevation with P-Wave Velocity

Figures

Figure 1-1	Location Map
Figure 1-2	Irish Hills 2011 2D/3D Seismic Acquisition Geometry
Figure 1-3	2014 Geologic Map and Data Compilation
Figure 2-1	2012 Phase 1 DCPD 3D Survey Source Layouts
Figure 2-2	2012 Phase 1 DCPD 3D Survey SigSeis Receiver Layouts
Figure 2-3	2012 Phase 1 DCPD 3D Survey SigSeis Receiver Layouts Detail
Figure 2-4	2012 Phase 1 DCPD 3D Survey Sources and Receiver Layouts Detail
Figure 2-5	Phase 2 3D Seismic Acquisition Geometry
Figure 2-6	2012 Zland Seismic Acquisition Geometry
Figure 2-7	Photographs of Obispo Formation Bedding in Discharge Cove
Figure 2-8	Sea-Cliff Exposure near the Rattlesnake Fault
Figure 3-1	Tectonic Map of the Los Osos–Santa Maria Domain
Figure 3-2	Strike and Dip Stereonet Plots for Obispo and Monterey Formations, South Limb Pismo Syncline
Figure 3-3	Complete Bouguer Gravity Anomaly Map
Figure 3-4	Potential Field Total Magnetic Intensity Anomaly Map (Helicopter)
Figure 3-5	Phase 1 Detailed Geologic Map
Figure 3-6	Explanation of the DCPD Site Specific Geologic Units
Figure 3-7	Photograph of Obispo Formation Bedding, Discharge Cove and Green Peak
Figure 3-8	Phase 2 Geologic Map

	FUGRO CONSULTANTS, INC <i>2012 Onshore Seismic Survey Report</i>	PR No.: PGEQ-PR-21
		Revision: 0
		Page 8 of 81

- Figure 3-9 Topographic Map of the Phase 2 Area, Showing Faults
- Figure 3-10 Location of Boreholes Drilled 1987–1989 in the Phase 2 Area
- Figure 3-11 Contour Map of the Wave-Cut Platform from Borehole and Outcrop Data, Rattlesnake Creek Area
- Figure 4-1 Characteristic Vp for Geologic Units in the South Irish Hills
- Figure 4-2 Location of Phase 1 VSD Tomography Lines
- Figure 4-3 Phase 1 Ray-Censored Tomography Line 1
- Figure 4-4 Phase 1 Ray-Censored Tomography Line 2
- Figure 4-5 Oblique View of the 12,500 Ft/s Isovelocity Surface, Irish Hills
- Figure 4-6 Phase 1 Ray-Censored Tomography Depth Slice at 358 Feet Below Sea Level
- Figure 4-7 Phase 1 Ray-Censored Tomography Depth Slice at 3 Feet Above Sea Level
- Figure 4-8 Comparison: Surface Geology and Total Magnetic Intensity Anomaly Helicopter Map
- Figure 4-9 Phase 1 Potential Field Total Magnetic Intensity Anomaly Map (Helicopter)
- Figure 4-10 Oblique View of the 2.50 g/cm³ Isodensity Surface, Irish Hills
- Figure 4-11 Location Map for Isovelocity Text Discussion
- Figure 4-12 Uninterpreted Phase 1 Filtered and Unfiltered Seismic-Reflection Profile Crossline 459, North-South
- Figure 4-13 SigSeis Crossline 458 High-Pass Filter Seismic-Reflection Profile with Tomography Overlay
- Figure 4-14 SigSeis Crossline 458 Rawstack Seismic-Reflection Profile with Tomography Overlay
- Figure 4-15 SigSeis Crossline 458 Rawstack Seismic-Reflection Panel, Interpreted
- Figure 4-16 Interpreted and Flattened Phase 1 Filtered Seismic-Reflection Profile Crossline 459, North-South
- Figure 4-17 Phase 1 SigSeis 2D Reflection Profiles with Vp Tomography Overlay, Lines 1 and 2
- Figure 4-18 Location Map, Phase 1 Reflection and Tomography Profiles
- Figure 4-19 Phase 1 SigSeis 2D Reflection Profiles with Vp Tomography Overlay, Lines 3, 4, and 5

	FUGRO CONSULTANTS, INC <i>2012 Onshore Seismic Survey Report</i>	PR No.: PGEQ-PR-21
		Revision: 0
		Page 9 of 81

Figure 4-20	Location Map for DCPV Vicinity Seismic-Reflection and Tomography Profiles
Figure 4-21	Phase 1 Reflection and Tomography Overlay Profiles 374, 375, and 376
Figure 4-22	Phase 1 Reflection and Tomography Overlay Profiles 377, 378, and 379
Figure 4-23	Phase 1 Reflection and Tomography Overlay Profiles 380, 381, and 382
Figure 4-24	Phase 1 Reflection and Tomography Overlay Profiles 383, 384, and 385
Figure 4-25	Phase 1 Reflection and Tomography Overlay Profiles 386, 387, and 388
Figure 4-26	Phase 1 Reflection and Tomography Overlay Profiles 389, 390, and 391
Figure 4-27	Phase 1 Reflection and Tomography Overlay Profiles 392, 393, and 394
Figure 4-28	Phase 1 Reflection and Tomography Overlay Profiles 395, 396, and 397
Figure 4-29	Phase 1 Reflection and Tomography Overlay Profiles 398, 399, and 400
Figure 4-30	Phase 2 Reflection-Amplitude with Vp Tomography Overlay, Profile A-A'
Figure 4-31	Schematic Cross Section of Marine Terrace Showing Depths of Reflection Slices
Figure 4-32	Phase 2 Profile Location Map
Figure 4-33	Phase 2 Tomography Slices at Elevations of 60 and -150 Feet
Figure 4-34	Phase 2 Tomography and Reflection Amplitude, Profile F-F'
Figure 4-35	Phase 2 4,900 Ft/s Isovelocity Surface
Figure 4-36	Phase 2 Boring Profile C-C' Top of Ks and 4,900 Ft/s Isovelocity Horizon
Figure 4-37	Phase 2 Boring Profile D-D' Top of Ks and 4,900 Ft/s Isovelocity Horizon
Figure 4-38	Phase 2 Boring Profile E-E' Top of Ks and 4,900 Ft/s Isovelocity Horizon
Figure 4-39	Phase 2 Reflection-Amplitude Slice 1, Depth Slice at 150 Feet Below Sea Level
Figure 4-40	Phase 2 Reflection-Amplitude Slice 2, Depth Slice at 60 Feet Above Sea Level
Figure 4-41	Phase 2 Reflection-Amplitude with Vp Tomography Overlay, Profile B-B'
Figure 4-42	Phase 2 Dip of Maximum Similarity, Depth Slice at 60 Feet Above Sea Level

	FUGRO CONSULTANTS, INC <i>2012 Onshore Seismic Survey Report</i>	PR No.: PGEQ-PR-21
		Revision: 0
		Page 10 of 81

- Figure 4-43 Phase 2 Dip of Maximum Similarity, Depth Slice at 150 Feet Below Sea Level
- Figure 4-44 Phase 2 Bedrock Reflection Surface
- Figure 4-45 Phase 2 Bedrock Reflection Surface, Detail
- Figure 4-46 Phase 2 Topographic Lineaments
- Figure 4-47 Phase 2 RTP First Vertical Derivative of the Magnetic Field

Appendix

- Appendix A Isovelocity and Isodensity Maps of the Irish Hills

ABBREVIATIONS AND ACRONYMS

2D	two-dimensional
3D	three-dimensional
AB 1632	Assembly Bill No. 1632
AGC	automatic gain control
AWD	accelerated weight drop
CCCSIP	Central Coastal California Seismic Imaging Program
CDP	common depth point
CIGs	common-image gathers
CPT	cone penetrometer test
DCPP	Diablo Canyon Power Plant
DEM	digital elevation model
FCL	Fugro Consultants, Inc.
ft	feet
ft/s	feet per second
FVD	first vertical derivative
GIS	geographic information system
GMP	Geologic Mapping Program
gpcc	grams per cubic centimeter
HESS	high-energy seismic source
Hz	hertz
ISFSI	independent spent fuel storage installation
ka	thousand years ago (<i>also</i> thousand years old)
km	kilometer(s)
LiDAR	light detection and ranging
LOSM	Los Osos–Santa Maria
LTSP	Long-Term Seismic Program
m	meter(s)
Ma	million years ago (<i>also</i> million years old)
mm/yr	millimeters per year



MSL	mean sea level
NRC	U.S. Nuclear Regulatory Commission
nT	nanotesla(s)
ONSIP	Onshore Seismic Interpretation Project
PG&E	Pacific Gas and Electric Company
PSDM	pre-stack depth migration
PSHA	probabilistic seismic hazard analysis
PTR	Participatory Technical Reviewer
P-wave	compressional seismic wave
QA	quality assurance
SLBP	San Luis Bay/Pismo structural block
S-wave	shear seismic wave
USGS	U.S. Geological Survey
V _p	P-wave velocity
V _s	S-wave velocity
VSD	vertical seismic display

	FUGRO CONSULTANTS, INC <i>2012 Onshore Seismic Survey Report</i>	PR No.: PGEQ-PR-21
		Revision: 0
		Page 13 of 81

1.0 INTRODUCTION

This report presents the results of a three-dimensional (3D) seismic survey campaign conducted at Pacific Gas and Electric Company's (PG&E) Diablo Canyon Power Plant (DCPP), located in San Luis Obispo County, California. This work is being done by PG&E to comply with the California Energy Commission's (CEC) recommendation, as reported in the CEC's November 2008 report titled *An Assessment of California's Nuclear Power Plants: AB 1632 Report*, that PG&E use 3D seismic-reflection mapping and other advanced geophysical techniques to explore fault zones near the DCPP.

Shallow high-resolution 3D seismic-reflection and seismic-velocity tomography data were acquired in the late summer and fall of 2012 for the purpose of locating and describing the geometry of buried geologic structures. PG&E contracted with Fugro Consultants, Inc. (FCL), to acquire, process, and interpret these data. This project is entitled the "2012 Onshore Seismic Interpretation Project" and is referred to herein as the "2012 ONSIP." This report documents the FCL mapping and assessment of the 2012 ONSIP data. The data consist of 3D seismic-reflection and P-wave tomography data volumes, associated pertinent 2011 reflection and tomographic data, and other supporting potential field geophysical data that FCL collected, processed, and interpreted for the Central Coastal California Seismic Imaging Program (CCCSIP) in the vicinity of the DCPP. The 2012 3D seismic data acquisition program was conducted in two phases, each phase covering a distinct geographic area (Figure 1-1).

The Phase 1 area consists of the DCPP and adjacent lands within approximately 1 kilometer (km) of the plant. Seismic survey data were collected up to 3 km from the plant, with detailed data collection and interpretation taking place within the 1 km radius (Figure 1-1). The Phase 1 area is also referred to as the "2012 3D DCPP volume." This area was selected for detailed study to address the requirement of U.S. Nuclear Regulatory Commission (NRC) Regulatory Guide 1.208, for very detailed geological and geophysical investigations within 1 km of a nuclear plant site.

The Phase 2 area consists of an approximately 0.5 km wide and 3.5 km long strip of coastal terraces located southeast of the DCPP (Figure 1-1). The Phase 2 area is also referred to as the "2012 3D marine terrace volume." This area was selected for detailed studies because mapped faults project through the area and the wave-cut bedrock platform beneath the marine terrace deposits may serve as a strain marker for Quaternary deformation associated with these faults. As these terraces have been placed in a time frame, this aspect of this study also places some age constraints on any structural features that deform the terraces.

The approach of this 2012 ONSIP study is to evaluate, map, and interpret the 2012 Phase 1 and Phase 2 high-resolution 3D seismic tomography and reflection data volumes honoring existing surface geologic mapping, geophysical, borehole, and potential field data. The existing data sets are integrated with the 2012 3D data volumes to map known,

	FUGRO CONSULTANTS, INC <i>2012 Onshore Seismic Survey Report</i>	PR No.: PGEQ-PR-21
		Revision: 0
		Page 14 of 81

and identify potential unknown surface geologic structures to depth within the lateral and vertical resolution of the seismic and tomographic data.

The interpretations presented in this report also draw on an extensive base of seismic survey data collected by PG&E and its contractors in the past 3 years, and geologic data collected over more than 25 years of study of this site. Recent data include the results of seismic surveys conducted onshore in 2011 and offshore in 2010, 2011, and 2012, an updated surface geologic map (PG&E, 2014a), and a study of the Shoreline fault (PG&E, 2011). Earlier data include geologic data collected in the 1980s for the Long-Term Seismic Program (LTSP) (PG&E, 1988, 1989a, b, 1990) and publications that resulted from these studies (Hanson et al., 1994; Lettis and Hall, 1994; Lettis et al., 1994, 2004; Page et al., 1998).

The 2011 two- and three-dimensional (2D/3D) program covered a wider regional area across the northern Irish Hills including Los Osos Valley (Figure 1-2). Interpretation of the 2011 Onshore Seismic Interpretation Project (2011 ONSIP) data is the focus of a separate report (PG&E, 2014b). The 2011 2D/3D seismic data acquisition was designed to acquire deeper crustal- and regional-scale seismic data across the Pismo syncline to evaluate geometries of geologic structures in the Irish Hills region, specifically, the major onshore surface-mapped faults (Los Osos, San Miguelito, Edna, and San Luis Bay), and to potentially identify other buried or blind structures in the region. The depth range of interest for 2011 2D/3D data was from the near surface to as deep as possible within the crust; effective maximum imaging depths of the 2011 Vibroseis data range from 4 to 8 km due to limits on available resolution of seismic velocities below 6 km and source-receiver offsets.

In contrast to 2011 2D/3D objectives, the 2012 3D seismic data acquisition was designed to acquire shallow, more detailed, and higher-resolution data for the DCP foundation area and proximal marine terraces. The seismic acquisition was designed to acquire data to provide seismic imaging in the depth range of interest for the shallow high-resolution 2012 ONSIP data of 0–1 km in the Phase 1 area and 0–0.25 km in the Phase 2 area.

The forthcoming PG&E report, *Central Coastal California Seismic Imaging Program Executive Summary*, will summarize the results and conclusions of the multiple onshore and offshore phases of the CCCSIP.

This report is organized as follows:

- Section 1 presents the background and history of the project, lists the data and reports that form the foundation for this report, reviews the project objectives and approach, describes the quality assurance parameters, and reviews the contracted scope of work.
- Section 2 summarizes the data collection and processing activities, referring the reader to previous data reports for complete documentation of these efforts. Limitations and uncertainties of the data are addressed.

	FUGRO CONSULTANTS, INC <i>2012 Onshore Seismic Survey Report</i>	PR No.: PGEQ-PR-21
		Revision: 0
		Page 15 of 81

- Section 3 reviews the geologic setting and provides the framework for interpretation of the seismic surveys. The section summarizes the regional geology and the geology of the Phase 1 and Phase 2 areas.
- Section 4 presents the data analysis, interpretation, and results, subdivided into Phase 1 and Phase 2 subsections. Each subsection reviews the nature of the data, describes the methods of analysis and interpretation, and presents both the uninterpreted and interpreted data.
- Section 5 summarizes the results and presents the conclusions of the study.
- Section 6 presents recommendations for further study.
- Section 7 lists all references cited.

1.1 Background

In 2006, Assembly Bill (AB 1632) was enacted, directing the California Energy Commission (CEC) to assess vulnerabilities of California’s base-load power plants to disruption from effects of plant aging and seismic events (State of California, 2006). The CEC prepared a report, *An Assessment of California’s Nuclear Power Plants: AB-1632 Report* which recommended that PG&E update its seismic hazard assessments for the DCP. The report recommended the use of 3D seismic acquisition and processing technologies (CEC, 2008).

In response, PG&E implemented the multi-year CCCSIP seismic data acquisition campaign to acquire seismic and other geophysical data in onshore and offshore areas surrounding the DCP. PG&E commissioned FCL to manage the data acquisition and processing of the 2011 and 2012 onshore and offshore campaigns. FCL was also asked to provide interpretation of the 2012 3D onshore seismic survey data.

The purpose of these combined efforts is to evaluate and measure downdip geometries of known surface faults and identify any previously unknown blind or buried geologic structures to provide data-informed constraints so that a 3D model can be made of the geologic structure beneath and adjacent to the DCP. This model can then be used to inform, constrain, and reduce uncertainties in the input parameters used in the DCP probabilistic seismic hazard analysis (PSHA).

As described in the previous subsection, the CCCSIP program began in 2011 with an extensive program to collect 2D and localized 3D data over a wide area of the northern Irish Hills and adjacent offshore areas (Figure 1-2). The purpose of this seismic survey campaign was to understand the larger structural setting, including the geometry of the major folds and faults.

At the close of the 2011 onshore and offshore seismic survey campaigns, PG&E made plans to collect detailed seismic survey data targeting specific areas, depths, and geologic structures. One element of the 2012 proposed project design was the “High-Energy Seismic Source” (HESS) project, which involved placing nearshore hydrophones along the shallow marine portions of the coastline in the study area to provide receiver coverage

	FUGRO CONSULTANTS, INC <i>2012 Onshore Seismic Survey Report</i>	PR No.: PGEQ-PR-21
		Revision: 0
		Page 16 of 81

in the nearshore transition zone in waters too shallow for offshore seismic sourcing. The HESS survey would increase receiver coverage across the Shoreline fault and provide continuous coverage between the offshore and onshore data volumes. Plans also included HESS offshore marine vessel-based high-energy offshore 3D acquisition “undershooting” the onshore live receiver arrays to provide high-energy long-offset shots into the onshore array.

Unfortunately, permits to use offshore high-energy sources were denied and this portion of the planned data acquisition was canceled. As a result, none of the 2012 CCCSIP data were acquired using high-energy offshore seismic sources, and no nearshore transition zone data were collected. The combined onshore-offshore seismic survey was designed to provide additional offshore aperture for complete 3D imaging of nearshore and onshore data. The cancellation of the offshore program reduced the extent and quality of onshore data acquired in the Phase 1 area near the coast by eliminating the offshore aperture necessary to attain complete 3D migrations in onshore areas near the coast. However, the term “high energy” remains as an artifact in the QA documents that govern the 2012 onshore seismic survey, as these documents (including the project planning document and the project instructions), had been prepared in advance.

The 2012 onshore program was designed to provide 3D detailed information in two critical areas: one area containing the DCPD and the other encompassing the San Luis Bay fault zone southeast of the DCPD.

Field acquisition for the 2012 3D onshore seismic survey data took place in the summer and fall of 2012. Processing of the data began in late 2012 and continued through 2013. FCL prepared a number of data reports to document these efforts and present the raw and processed data. The data reports form the foundation for the synthesis and analysis presented in this project report. The pertinent data reports are listed below in order by project number:

- PGEQ-PR-07: Validation of the Commercial Software IHS Kingdom Version 8.6 Hotfix 4 2d/3dpak, Vupak, and Rock Solid Attributes (FCL, 2012).
- PGEQ-PR-08: 2011 and 2012 Data Processing Report (FCL, 2014a).
- PGEQ-PR-14: CCCSIP Onshore 2012 Data Report (FCL, 2013a).
- PGEQ-PR-16: DCPD P- and S-Wave Foundation Velocity Report (FCL, 2014b).
- PGEQ-PR-17: 2012 PG&E P-Cable Low-Energy Seismic Survey, 3D Data Processing Report, San Luis Bay (FCL, 2013b).
- PGEQ-PR-18: 2012 PG&E P-Cable Low-Energy Seismic Survey, 3D Data Processing Report, Point Sal (FCL, 2013c).
- PGEQ-PR-19: 2012 PG&E P-Cable Low-Energy Seismic Survey, 3D Data Processing Report, Estero Bay (FCL, 2013d).
- PGEQ-PR-20: QA Documentation for 2012 ONSIP Data Processing and Interpretation (FCL, 2014c).

	FUGRO CONSULTANTS, INC <i>2012 Onshore Seismic Survey Report</i>	PR No.: PGEQ-PR-21
		Revision: 0
		Page 17 of 81

- GEO.DCPP.TR.14.03: ONSIP 2011 Data Report: Report submitted to the U.S. Nuclear Regulatory Commission (PG&E, 2014b).

1.2 Objectives and Approach

The overall objective of the 2012 ONSIP was to image the location and geometry of subsurface geologic structures such as faults and folds within the Phase 1 and 2 areas. Specific targets included known or suspected faults, but the identification of previously unknown structures was also anticipated.

For both the Phase 1 and Phase 2 areas, the approach was to use 3D seismic survey methods to collect high-quality and high-resolution subsurface data. The 2012 data collection program was designed to obtain high-resolution 3D data at the locations and depths most appropriate for the anticipated structure and geology of each of these two areas.

Once the data were collected and processed, as detailed in the 2013 data report (FCL, 2013a), the processed data were imported into IHS Kingdom (Version 8.6 HF4) software, allowing the data to be visualized in 3D, and structures to be interpreted and mapped. Constraints from existing geologic mapping, well and borehole data, gravity data, and magnetic data were incorporated into the interpretations.

1.2.1 Phase 1 Objectives and Approach

The 2012 3D Phase 1 acquisition program was designed to address the NRC's Regulatory Guide 1.208 requirement that "very detailed geological, geophysical, and geotechnical investigations" be performed within 1 km of a nuclear site location to assess specific soil and rock characteristics" (Figure 1-1). Specific goals of the 2012 Phase 1 program were to evaluate the downdip subsurface geometries of known geologic structures, investigate the nature of mapped queried or inferred lineaments surrounding the DCP (PG&E, 2014a), and to describe the relationship between surface geologic mapping and the new subsurface seismic imaging. In addition, P-wave and S-wave tomography volumes were processed for reflection processing inputs and DCP foundation P-wave and S-wave velocity analyses, described in the FCL Foundation Velocity Report (FCL, 2014b).

Specific targets in the Phase 1 area included the San Miguelito fault zone within the data extent as mapped at the surface and as projected along strike, mapped structures in the vicinity of the DCP in Discharge Cove, Unnamed Cove, and Intake Cove, a detailed fault presence/absence assessment in the vicinity of the DCP, any blind or previously undetected structures, and any structures that may step offshore toward the Shoreline fault.

1.2.2 Phase 2 Objectives and Approach

The 2012 Phase 2 objectives were to constrain the location, geometry, and displacement of traces of faults splaying from the San Luis Bay fault system. These faults, presently

	FUGRO CONSULTANTS, INC <i>2012 Onshore Seismic Survey Report</i>	PR No.: PGEQ-PR-21
		Revision: 0
		Page 18 of 81

shown as uncertain, approximate, or inferred fault traces on the geologic map (Figure 1-3 and 1-4; PG&E, 2014a), cross the coastal terraces and project offshore toward lineaments mapped in the bathymetric data (PG&E, 2012). The Phase 2 acquisition program was designed to image the top of the bedrock platform, and the structure of the shallow bedrock, beneath unconsolidated Quaternary sediments of the marine terraces. The premise is that any linear deflections in the bedrock surface revealed by the seismic survey may indicate the presence of one of these faults. In addition, structures within the bedrock may be imaged.

Specific targets in the Phase 2 area were mapped fault structures including the Olson, Rattlesnake, and San Luis Bay structures and associated features that reflect bedrock offset and potential offset of Quaternary sediments, and a first-pass assessment of any blind or previously undetected structures.

The primary approach in the Phase 2 area was to calibrate the tomographic model with existing geologic data, then extrapolate the tomographic model so as define the shape of the bedrock surface beneath the terrace sediments. Existing data in the Phase 2 area are published in previous geologic studies by PG&E (1989a, 1990), Hanson et al. (1994), and Lettis et al. (1994). In the late 1980s, PG&E drilled and logged 142 shallow soil borings along the terraces between Point Buchon and Pismo Beach to determine the elevation and geometry of the bedrock marine platforms (PG&E, 1989a, 1990). Fifty-five of the borings lie within the Phase 2 area, and most encounter Cretaceous sandstone bedrock beneath Quaternary sediments.

The spatially referenced borehole data were digitally imported into the seismic interpretation software (IHS Kingdom Version 8.6 HF4) to calibrate the vertical depth resolution of the seismic volume. In combination, the borings and seismic-reflection data are used to generate a sub-crop map showing the top of Cretaceous sandstone bedrock beneath the Quaternary sediments to evaluate deformation in the emergent marine terrace surface, an originally planar datum. Any potential terrace surface offset location would become a candidate for further ground-based paleoseismic investigations.

A secondary approach, undertaken to identify structures in the underlying bedrock, was to map planar features identified in the seismic-reflection volume, then evaluate these planes as possible faults, bedding planes, or joints. This approach would potentially confirm the presence, geometry, and location of known faults, and help identify previously unknown faults or other structures.

1.3 Quality Assurance

This section describes FCL's Quality Assurance (QA) program for this project and presents the contracted scope of work for the analysis and interpretation of the 2012 3D onshore seismic survey data.

	FUGRO CONSULTANTS, INC <i>2012 Onshore Seismic Survey Report</i>	PR No.: PGEQ-PR-21
		Revision: 0
		Page 19 of 81

1.3.1 NQA-1 Program

This work is considered a nuclear safety-related activity, thus was conducted in strict conformance with the FCL NQA-1 Quality Assurance (QA) program. In addition, all work performed by FCL and its subcontractors was reviewed and approved by the PG&E QA and technical project management teams. Complete QA documentation for the 2012 3D seismic survey project is provided in a separate report, PGEQ-PR-20 (FCL, 2014c).

The primary FCL QA document prepared to govern the work presented in this report is the project instruction, PGEQ-PI-16, Revision 0, “Geophysical Interpretation and Reporting of 2012 3D Seismic Data: Work Element 2, Phase 3,” dated 29 October 2013 and pursuant to project planning document PGEQ-PPD-001.

The 2012 data collection and interpretation effort was conducted at the request Dr. Stuart Nishenko, PG&E Geosciences Department, with PG&E QA oversight by Ms. Marcia McLaren. FCL provided technical oversight for the data collection and processing effort, and carried out the geologic interpretation tasks presented in this report. The FCL team worked closely with Nishenko and McLaren throughout the project.

1.3.2 Scope of Work

This project report constitutes a required deliverable under the Scope of Work described in PG&E CWA No. 350095480 Rev. 3 to FCL, issued 23 October 2013. PG&E’s review comments have been incorporated, and Revision 0 of this report represents the final deliverable associated with this CWA. Data interpretation and seismic mapping activities are summarized herein.

The above-referenced CWA specified the following tasks under the scope of work:

- **Task 1:** Quality Assurance Activities and Management. This is a QA task, which includes the following activities:
 - Adoption of existing and/or preparation of new QA documents.
 - Review.
 - QA training.
 - Coordination with the PG&E Geosciences QA Manager.
- **Task 2:** 2012 3D Seismic Data Stratigraphic Mapping. This is a QA task, which includes mapping of seismic stratigraphy in the 3D volumes, as follows:
 - For the 2012 DCPD 3D volume, this includes mapping first-order seismic stratigraphy in the volume consisting primarily of unit-basin boundaries and intrusive bodies with ties to surface geology and available boring logs.
 - For the 2012 Marine Terrace 3D volume, this includes mapping top of bedrock using surface geology and available boring logs.
- **Task 3:** 2012 3D Seismic Data Fault Mapping. This is a QA task that involves 3D mapping of the DCPD volume and the marine terrace volume.

	FUGRO CONSULTANTS, INC <i>2012 Onshore Seismic Survey Report</i>	PR No.: PGEQ-PR-21
		Revision: 0
		Page 20 of 81

For the 2012 DCPD 3D volume:

- The San Miguelito fault zone within the data extent as mapped at the surface and as projected along strike.
- Mapped fault structures in the “Southwestern Boundary zone,” including the Olson, Rattlesnake, and San Luis Bay structures and associated features that may step offshore toward the Shoreline fault.
- Unnamed mapped structures in the vicinity of Discharge Cove, Unnamed Cove, and the DCPD.
- Detailed fault presence/absence assessment in the vicinity of the DCPD.
- First-pass assessment of any blind or previously undetected structures.

For the 2012 marine terrace 3D volume:

- Assessments of mapped fault structures in the “Southwestern Boundary zone” including the Olson, Rattlesnake, and San Luis Bay structures and associated features in terms of bedrock offset and potential offset of soil.
- First-pass assessment of any blind or previously undetected structures.

The CWA further specified that work will be evaluated by a Participatory Technical Reviewer (PTR), identified and chosen by FCL in coordination with Stuart Nishenko of PG&E. James W. Granath, a structural geologist with Dynamic Upstream E&P Consultants, was chosen. Granath consulted with the team throughout the data analysis and interpretation phases of the project, and provided review comments on this report.

1.3.3 Safety-Related Software

Nuclear Safety-related software used in analysis and interpretation activities included IHS Kingdom Version 8.6 Hotfix 4 2d/3dpak, Vupak, And Rock Solid Attributes, The software was validated in conformance with FCL QA Procedure QAP-03C, and documented in report PGEQ PR-07, (FCL, 2012).

	FUGRO CONSULTANTS, INC <i>2012 Onshore Seismic Survey Report</i>	PR No.: PGEQ-PR-21
		Revision: 0
		Page 21 of 81

2.0 ONSHORE 2012 3D DATA ACQUISITION

The 2012 onshore field seismic surveys involved a full team of land seismic survey crews, multiple recording instruments, seismic-wave generating sources, and instrument calibration and testing protocols. Sources utilized during the seismic surveys included Vibroseis trucks, accelerated weight-drop (AWD), and sledgehammer impact sources. Detailed documentation of the 2012 data acquisition process is provided in a 2013 data report, PGEQ-PR-14, Revision 0, *CCCSIP Onshore 2012 Data Report* (FCL, 2013a).

This section summarizes the data collection activities in the Phase 1 and Phase 2 areas, and then addresses data resolution and the limitations inherent in these data.

2.1 Phase 1 Data Acquisition

The Phase 1 2012 data acquisition was designed to image subsurface geologic structures within approximately 1 km of the plant (Figure 1-1), and thus provide geometric constraints connecting mapped surface geologic features to likely subsurface features. The Phase 1 data set provides its highest resolution in the zero to 1 km depth range. Geologic features of primary interest are stratigraphic contacts, unconformity surfaces, fault surfaces (if present), associated potential fault dips, and potential fault intersections.

For a detailed account of Phase 1 2012 3D seismic acquisition parameters, recording equipment, and sourcing parameters, please see the PGEQ-PR-14 data report (FCL, 2013a).

The Phase 1 seismic survey data were acquired using a network of sources and receivers spread out across the area. Vibroseis sources were used for the Phase 1 acquisition. Three types of seismic recording systems, or receivers, were employed:

- Seistronix
- Sigma
- Nodal Zland

The more closely spaced Sigma and Seistronix data were combined into the “SigSeis” 3D volume. (“SigSeis” is a contraction that designates combined Sigma and Seistronix data.) The more widely spaced Zland data were primarily utilized to generate a 3D high-resolution P-wave tomography volume. Layouts of the Phase 1 sources and receivers, both SigSeis and Zland are illustrated on Figures 2-1 through 2-4.

Seismic sourcing in the Phase 1 area was prohibited immediately adjacent to and within specific large structures within the DCPD and over most of the “San Luis Obispo 2” archaeological site area located on the marine terraces northwest of Diablo Creek; seismic sourcing was permitted in narrow corridors within the DCPD defined by a vibration control plan. Another spatial restriction on the seismic sourcing was that sourcing was mostly only permitted along existing roads; overland grids of seismic sourcing were limited to a few areas. This permitting restriction severely limited the

	FUGRO CONSULTANTS, INC <i>2012 Onshore Seismic Survey Report</i>	PR No.: PGEQ-PR-21
		Revision: 0
		Page 22 of 81

sourcing to receiver coverage in the Phase 1 reflection survey. The 3D receivers were laid out over a larger area, but large gaps in receiver coverage exist in inaccessible portions of the Phase 1 area where receivers could not be logistically deployed, primarily in locations with very steep terrain and existing nuclear power generating facilities. This irregular 3D acquisition geometry, due to source location permit constraints and irregular receiver deployment, did not allow for traditional inline and crossline receiver deployment and infilling the grid with regular source shot points at each inline and crossline half-space location. Implications and limitations resulting from the irregular Phase 1 acquisition geometry are discussed in greater detail in Section 2.3.

2.2 Phase 2 Data Acquisition

The Phase 2 data set was collected in 2012 on the marine terraces southeast of the DCP (Figure 1-1). The survey was designed to have the highest resolution in the 0 to 800 feet (ft) (0 to 250-meter (m)) depth range. Phase 2 seismic acquisition was performed with tightly spaced 5 m inline and 10 m crossline source-receiver spacing recorded by a Seistronix system using Vibroseis sourcing with one to two EnviroVibe vibrators at half station spaces. Ideal 3D receiver and sourcing inline-crossline geometries were permitted for the Phase 2 area. Phase 2 data collection activities on the marine terraces southeast of the DCP involved the Seistronix and the Sigma recording systems. Layouts of sources and receivers in the Phase 2 area are shown on Figure 2-5.

The Phase 2 seismic acquisition geometry was an ideal 3D configuration, which used a rectangular grid with 5 m inline and 10 m crossline source-receiver spacing. The Phase 2 acquisition was designed to obtain well-resolved acoustic imaging of shallow (~10–750 ft depth) subsurface structure along the coastal terrace (Figure 2-5). The 3D reflection data volume was post-processed to generate two depth-migrated 3D seismic-amplitude volumes: a raw (unfiltered) volume and an automatic gain control (AGC) filtered volume. The raw, unfiltered reflection-amplitude volume, along with the derivative seismic-attribute data volumes (e.g., dip of maximum similarity) generated from the raw unfiltered data, was preferred for 3D mapping in this study; the raw data preserve relative reflection amplitudes and contain fewer processing artifacts relative to the AGC volume. Bin spacing for both volumes is 16 ft in the inline direction and 8 ft in the crossline direction; both achieve a bedding resolution of approximately 6 ft near the base of soil to 30 ft in rock below the weathering zone (Table 2-1). Vertical fault offsets are detectable at about one-half of the bedding resolution, approximately 3–15 ft, but consistent resolution of faulting requires vertical fault offsets of at least 5 ft in soil and 20–25 ft in rock below the weathering zone.

The original Phase 2 data acquisition was planned to extend farther to the northwest across Olson Hill to image the extent of the San Luis Bay fault where it bends across the terraces and extends offshore. Due to schedule, budget, and permitting restrictions, the Phase 2 data acquisition was halted southeast of this area, and no seismic data were

	FUGRO CONSULTANTS, INC <i>2012 Onshore Seismic Survey Report</i>	PR No.: PGEQ-PR-21
		Revision: 0
		Page 23 of 81

acquired to characterize the San Luis Bay fault in the vicinity of Olson Hill (Figure 2-5). Therefore, this fault segment could not be assessed.

2.3 Resolution and Limitations of the Seismic Survey Data

Details of the data acquisition, processing, and characteristics are presented in this section. The 2012 Phase 1 and Phase 2 3D seismic survey data are subject to a number of limitations that govern the degree to which they will be able to effectively image subsurface structures. This chapter provides pertinent and important discussion on the limiting aspects, areas of data resolution, and the physical resolution limits of these seismic data. These limitations should be understood before reading the data assessment and interpretation chapters.

Seismic survey methods are most easily applied to relatively flat-lying sedimentary strata, and are not particularly useful for imaging complexly deformed strata, metamorphic, igneous, and acoustically quiet basement rocks. The Irish Hills consist of all of these aforementioned geologic complexities. Other limitations result from non-ideal conditions for data collection, such as limited acquisition coverage, limited source or receiver density, or non-ideal layout geometry. This is to be expected within the Phase 1 area, which contains the DCP, an operating power generating facility with large building structures and power transmission areas that were inaccessible for seismic data acquisition. Other limitations result from a lack of deep downhole geophysics and geologic logs.

Data interpretability is complicated by the complex geology of the study area, which is comprised of folded Tertiary Obispo sedimentary strata, and metamorphic (Franciscan Formation) and igneous rocks (Obispo Formation diabase intrusives). So, end users of these 2012 3D seismic-reflection data should remember that typically, metamorphic and igneous rocks exhibit acoustic reflectivity that appears as acoustically quiet, with internal reflectivity ranging from simple to highly complex and irregular.

Seismic-reflection data image velocity heterogeneity (acoustic impedance contrasts), and as such are acoustic images. The degree to which they faithfully or literally represent geologic images is sometimes taken for granted. For example, seismic-reflection data collected over a homogeneous material with uniform velocity and density would show no seismic-reflection signals. Geologic stratigraphy that consists of regular sequences of juxtaposed fast and slow geologic units, with thicknesses greater than a quarter of a seismic wavelength, yield the most geologically faithful seismic images. This fidelity decreases with increasing stratigraphic and structural complexity.

The 2012 3D seismic-reflection survey data acquisition geometry, or relative source and receiver locations, determines the spatial extent and resolution of subsurface imaging. Seismic-reflection imaging is typically focused over a particular depth range, and effective and efficient data acquisition requires the use of acquisition geometry specifically engineered to obtain quality imaging within the particular target depth range.

	FUGRO CONSULTANTS, INC <i>2012 Onshore Seismic Survey Report</i>	PR No.: PGEQ-PR-21
		Revision: 0
		Page 24 of 81

The Phase 1 DCPD 3D seismic-reflection acquisition was designed to image from depths of 50–100 ft (~15–30 m) to 3,000–6,000 ft (~1,000–2,000 m). The large power-generating facilities and supporting building structures at DCPD limited source-receiver access. Complete coverage was not possible over dimensions on the order of 330 ft (~100 m) or more in parts of the Phase 1 survey area. “Undershooting,” or using receivers to record distant shot points, was the only strategy that could image beneath significant portions of the DCPD. Consequently, Phase 1 data acquisition was designed with nominal 32.8 ft (10 m) source-receiver spacing near the DCPD to obtain as much near-offset data as was feasible in and near the DCPD. However, there were portions of the Phase 1 survey area where receivers and sources could not be deployed due to facility and restricted zone locations, which resulted in data acquisition gaps on the order of 100–600 ft (30–200 m). Permitted Phase 1 source regions were primarily confined to roads and paved surfaces resulting in an irregular 3D acquisition geometry that precluded near-offset shallow 3D imaging in areas, locally resulting in irregular azimuthal-offset coverage in portions of the Phase 1 3D volume.

The Phase 2 marine terrace data acquisition was accomplished with regular orthogonal source-receiver grids and provided conventional 3D seismic imaging coverage over depths of 16.4 ft (5 m) to about 820 ft (250 m).

2.3.1 Phase 1 DCPD 3D Data Acquisition Impacts

As described in Section 2.1, three types of seismic receivers were used for the 2012 3D Phase 1 high-resolution seismic-reflection data acquisition: Sigma, Seistronix, and Zland (Figures 2-1, 2-2, 2-3, 2-6, and 2-7). The Sigma and Seistronix receivers used geophone groups of four geophones to improve signal-to-noise. The Zland receivers used a single geophone and were placed at coarser receiver group spacing (10–30 m). The coarser Zland receiver coverage does not provide shallow reflection imaging-resolution quality comparable to the Sigma and Seistronix data. Instead, the Zland data were primarily used to provide travel-time constraints over a larger area than the densely spacing Sigma and Seistronix receiver deployment extents. The increased Zland spatial coverage was designed to increase the maximum depth extent of 3D Vp tomographic imaging, and to ensure high-resolution tomographic imaging over the entire extent of the high-resolution seismic-reflection imaging volume.

The SigSeis receivers were deployed at a finer spacing (5–10 m), and data records from both receiver types were combined and processed as the “SigSeis” 3D seismic-reflection volume. The Seistronix receiver deployment was concentrated in the area north of Diablo Creek where seismic sourcing could only be performed on roads, and provided a fixed, roughly 800-channel 3D seismic array that recorded nearly all the seismic source points.

The Sigma recorders were “rolled,” or continuously moved and redeployed proximal to the seismic source points, to ensure high-density receivers recorded at near-offset to improve shallow imaging in areas where seismic sourcing activities were permitted. At any one time more than 1,200 Sigma channels were live during seismic sourcing. The

	FUGRO CONSULTANTS, INC <i>2012 Onshore Seismic Survey Report</i>	PR No.: PGEQ-PR-21
		Revision: 0
		Page 25 of 81

Sigma channels were migrated across the site over the duration of sourcing activities resulting in over 4,400 unique Sigma receiver locations. The combined SigSeis receiver deployment spanned more than 5,000 unique receiver positions; the Zland receivers occupied less than 3,000 unique receiver locations over a much larger area. Thus, the SigSeis volume provides the highest resolution 3D seismic-reflection imaging in the Phase 1 area within 1 km of the DCP, and is presented and interpreted herein. Comprehensive technical details of the reflection and tomographic processing are detailed in PGEQ-PR-08 (FCL, 2014a), and pertinent points on data acquisition and processing are discussed herein.

The acquisition geometry for the SigSeis 3D volume is shown on Figures 2-1, 2-2, 2-3, and 2-7. Figure 2-1 shows the extent of Vibroseis source locations. Each red dot on the Figure 2-1 map represents a Vibroseis seismic source shot, or shot point. All the receivers that were live recorded each shot point. Once all the receivers were deployed to their maximum extents, over 4,000 live receivers recorded individual shot points. There were large inaccessible areas including parking lots, building structures, and steep hill slopes where receivers were not deployed due to logistical, safety, or permit restrictions, resulting in several large (>100 m) gaps in comprehensive receiver coverage (Figures 2-1, 2-2, and 2-3). The region north of the DCP achieved the most consistent and highest-density 3D receiver coverage.

In contrast to the extensive 3D receiver deployments, 3D source point areas were limited to a small number of open field areas, and otherwise occurred only on roads or parking lots (Figure 2-1). One of the more extensive 3D sourcing areas was located in open fields north of Diablo Creek (Figure 2-1). The irregular 3D acquisition geometry is the result of cultural and environmental permitting restrictions that precluded off-road Vibroseis source operations over significant fractions of the entire Phase 1 area. Safety evaluations and strict adherence to a vibration control plan, required while working within the protected area of the DCP, precluded the operation of Vibroseis sources in some areas, which directly limited seismic source density and regularity that could be achieved within and close to the DCP. As a result, azimuthal and incidence angle coverage is erratic and incomplete within portions of the “SigSeis 3D Data Extent” polygon (Figures 2-1 through 2-4), particularly at depths less than 300 ft. The limited 3D distribution of source points places limits on 3D subsurface imaging coverage, particularly with respect to shallow imaging. Shallow imaging of rock structure below soil and shallow acoustic weathered zones at depths of 50 ft or more is limited to areas with nearby source coverage. Undershooting provides more consistent imaging at depths of 100–200 ft or more throughout much of the 3D SigSeis volume. Figure 2-4 provides a detail of the SigSeis receiver and Vibroseis source coverages.

2.3.2 Phase 1 DCP 3D Data Processing and Outputs for Interpretation

The SigSeis data were processed as a 3D volume using processing methods including 3D high-resolution tomography, 3D Fast Beam Migration (FBM), and prestack-depth-

	FUGRO CONSULTANTS, INC <i>2012 Onshore Seismic Survey Report</i>	PR No.: PGEQ-PR-21
		Revision: 0
		Page 26 of 81

migration velocity updates (FCL, 2014a). While the SigSeis 3D reflection volume was output as a regular 3D volume with 30 ft horizontal bin spacing and 15 ft vertical sampling, it is not an ideal, regular 3D volume. Standard 3D acquisition approaches utilize regular sourcing and receiver coverage acquired along inlines and crosslines that form a regular grid of receivers and source points, where each receiver location is near a shotpoint location. In the case of the SigSeis volume, the best imaging lies along portions of the 3D volume with both source shotpoints and receivers in the inline direction and a balance of source and receiver points distributed on both sides of the inline position. Therefore, in many areas of the SigSeis 3D volume, it is not possible to perform standard 3D seismic data interpretation; “standard 3D seismic data interpretation” being defined as the entire 3D data volume being well-constrained by regular acquisition geometry, and therefore the entire volume is interpretable.

In the Phase 1 SigSeis 3D volume as a whole, it is not appropriate to run 3D seismic attributes (e.g., similarity, coherency, or dip of maximum similarity), to interpret depth slices of the entire 3D volume, or to interpret any and every inline, crossline, or “arbitrary” line location throughout the entire 3D volume, as is standard with 3D volumes acquired and processed with regular source and receiver geometry. Multiple attempts and approaches were pursued during this reporting effort to run attributes, map the entire 3D volume, map in depth slices, and to generate structure contour maps of horizon surfaces throughout the volume, although ultimately these approaches proved unviable. The irregular acquisition geometry of the 3D volume limits the interpretability of the data to smaller 3D subsets and certain 2D alignments.

The limits on source point distribution were compensated somewhat by moving the Sigma receivers and reoccupying source points proximal to areas with new Sigma receiver array positions to improve near-offset 3D azimuthal coverage. This was time- and labor-intensive, but regularized the irregular acquisition geometry enough to provide valuable azimuthal and incidence angle infill for 3D processing. The resulting SigSeis 3D volume provides seismic imaging along select 2D profiles, extracted from the 3D volume, that are clearly superior to 2D acquisition alone. For example, 2D profiles extracted from the 3D volume along 2D crooked lines from the 2011 data acquisition show that the 2011 2D processed crooked lines, located within the 2012 SigSeis 3D volume, are often dominated by out-of-plane energy that crosscuts and sometimes completely obscures primary reflectors. Even 2D straight lines only record source points in the inline orientation. 2D acquisition completely lacks the added azimuthal and incidence angle coverage provided by crossline source locations, and, as a result, 2D migrations are incomplete. Consequently, the 2D profiles extracted from the 3D SigSeis volume are better constrained, higher resolution, and more completely migrated relative to data acquired in 2D alone, because of the addition of crossline migration in the 3D processing.

“Vertical seismic displays” (VSDs), or 2D vertical slices extracted from the 3D seismic volume, can be utilized to pull 2D VSD profiles in the SigSeis Phase 1 3D volume along

	FUGRO CONSULTANTS, INC <i>2012 Onshore Seismic Survey Report</i>	PR No.: PGEQ-PR-21
		Revision: 0
		Page 27 of 81

areas with both receiver and sourcing coverage. It is imperative that seismic interpreters fully understand the seismic acquisition geometry with respect to the resulting post-processed SigSeis 3D reflection volume, and only perform detailed interpretation along 2D VSD alignments in the 3D volume with adequate sourcing and receiver coverage along the alignment. The interpreter must recognize regions along the alignment where shallow imaging is absent where gaps in sourcing positions exist along the alignment.

Small subsets of the SigSeis volume with optimal 3D inline-crossline receiver coverage and sourcing could be extracted for processing smaller volumes of 3D seismic attributes, such as the area of dense coverage the northwestern portion of the SigSeis 3D data coverage extent, in the event that future detailed investigations are pursued in this vicinity.

The amplitudes returned from the prestack-depth migrations of the 2012 Phase 1 SigSeis data were used unmodified in the stacks that produce the final Phase 1 3D seismic-reflection volume (FCL, 2014a). Consequently, reflectivity variations within the volumes are proportional to the scale of velocity contrasts across reflectors because automatic gain control filtering was not used after stacking of the migration amplitudes. This final stage of relative reflector amplitude preservation is very important: it allows interpreters to recognize and differentiate more reflective sequences of seismic strata commonly associated with sedimentary stratigraphy from relatively low reflectivity regions associated with acoustically quiet and/or reflectively chaotic basement rocks.

2.3.3 Phase 2 Marine Terrace 3D Impacts of Data Acquisition and Processing

A regular 3D geometry of sources and receivers was used with a 16.4 ft (5 m) inline receiver spacing in the north-south direction and a 32.8 ft (10 m) crossline receiver spacing. EnviroVibe source points also used a 16.4 ft (5 m) inline spacing and a 32.8 ft (10 m) crossline spacing. Source points were offset 5 m in the crossline direction to create a regular 5 m grid of combined source and receiver locations in the inline and crossline directions. The total number of live receivers varied from about 800 to over 2,000 depending on the width of the terrace in the live spread. Over 12,000 source and receiver positions were occupied in total (Figure 2-5).

The 3D high-resolution tomography provided velocities and statics for the seismic-reflection processing and the final output of a Kirchhoff 3D prestack-depth migrated 3D volume (FCL, 2014a). The raw migrated amplitudes were stacked to preserve relative amplitudes throughout the volume. The 3D seismic-reflection volume was output using an 8 ft (2.4 m) inline bin spacing and 16 ft (4.9 m) crossline bin spacing, a vertical sampling of 2 ft (0.6 m), and was trimmed to an extent confined to the source-receiver deployment extents (Figure 2-5). The regular data acquisition geometry and 3D processing provide a regular 3D seismic-reflection volume suitable for full 3D interpretation including calculation of 3D attributes over the 16.4–820 ft (~5–250 m) depth range.

	FUGRO CONSULTANTS, INC <i>2012 Onshore Seismic Survey Report</i>	PR No.: PGEQ-PR-21
		Revision: 0
		Page 28 of 81

2.3.4 3D Seismic-Reflection Resolution and Depth Extent

The frequency bandwidth of the seismic sourcing and recorded reflection data, the spatial sampling of the data acquisition, and the seismic velocity structure determine the fundamental limits on seismic-reflection resolution, including the minimum feasible depth of effective seismic-reflection imaging. Furthermore, the maximum depth of consistent seismic imaging is limited by aperture of data acquisition and the dip of seismic reflectors in the deeper portion of the volume. The following sections define these limitations for the Phase 1 and Phase 2 areas, which have different data resolutions and depth extents directly related to the unique acquisition geometries of each area.

2.3.4.1 Phase 1 Seismic-Reflection Resolution and Depth Extent

Phase 1 SigSeis 3D data were acquired with a nominal source-receiver spacing of 10 m, an effective center frequency of 40 Hz in a seismic bandwidth of 20–80 Hz, and typical shallow rock velocities of 6,400 ft/s, the depth of quarter wavelength corresponds to 40 ft. Thus, for the Phase 1 SigSeis 3D volume, the minimum mute (depth of zeroing from topography to depth in the 3D volume) is about 40 ft, and is as large as 300 ft in areas where seismic source points were more than 1,000 ft from nearby receiver groups.

The maximum depth of consistent seismic imaging is limited by aperture of data acquisition and the dip of seismic reflectors in the deeper portion of the volume. For the Phase 1 SigSeis 3D volume, the widest aperture outside the 3D imaging extent was obtained to the north and east of the acquisition volume, improving the imaging potential of deeper north-northeast dipping units. Seismic sourcing was conducted out to offsets of approximately 6,000 ft (~2 km) north, east, and south of the center of mass of the SigSeis receiver arrays to provide offsets, and thus migration aperture, that are about two times larger than the maximum imaging depth of 3,000 ft (~1 km; Figures 2-1 through 2-4).

The maximum consistent imaging depth of the Phase 1 SigSeis 3D volume is approximately 3,000 ft (~1 km). The HESS onshore-offshore program (that was canceled) was designed to complete the migration aperture into the offshore region. Consequently, a caveat of the Phase 1 SigSeis 3D volume is that depth imaging becomes more uncertain for the deeper portion of the volume (~1,000–3,000 ft) close to the coast, since migration aperture is incomplete for any reflectors that would be dipping southwest.

The broad distribution of 2012 Zland receivers (Figure 2-6) provided critical velocity constraints for the Phase 1 seismic-reflection processing for the 3D Vp tomography volume coverage area. Well-constrained acoustic velocities were extended approximately 6,000 ft (~2 km) beyond the onshore limits of the 3D SigSeis volume. The resulting high-resolution 3D tomography volume provided well-constrained velocities to migrate long-offset sourcing outside of the SigSeis receiver coverage. The tomography coverage provided important constraints that achieved the aperture necessary to image to approximately 3,000 ft (~1 km) depth in the 3D SigSeis volume.

	FUGRO CONSULTANTS, INC <i>2012 Onshore Seismic Survey Report</i>	PR No.: PGEQ-PR-21
		Revision: 0
		Page 29 of 81

Only a few iterations of prestack-depth-migration (PSDM) velocity analyses and velocity updates were needed to confirm that only small adjustments of the Phase 1 high-resolution 3D tomographic velocities were necessary to flatten reflectors in common-image gathers (CIG). Confirmation of flat reflectors in PSDM CIGs is the most important and objective data processing criteria to assess the accuracy of the depth migration. Additional confirmation of the accuracy and consistency of Phase 1 SigSeis 3D volume depth imaging is the one-to-one spatial correspondence (depth and horizontal positions) of strong reflectors with large velocity contrasts in the 3D tomographic model as shown in velocity overlays on the seismic-reflection depth sections, presented in Section 4.1.6.

In the Phase 1 SigSeis 3D volume, the seismic-reflection resolution limits are determined by the frequency bandwidth of the reflection data (40 Hz central frequency, 80 Hz maximum frequency), the 3D binning (30 ft horizontal bins, 15 ft vertical sampling), the local regularity of the 3D data acquisition geometry, and the typical seismic velocities in shallow unweathered rock (approximately $\leq 8,000$ ft/s). Bedding resolution is 25 ft or larger as velocities increase, based on a quarter wavelength criteria. Resolution of vertical deflection of bedding is 15 ft or larger, based on the limits of discernable deflection of quarter wavelength bedding. Minimum horizontal wavelengths of resolvable folding are on the order of 200 ft or more in shallow regions, and increase with increasing velocity to wavelengths of 400 ft or more at 500–1,000 ft depths.

Phase 1 SigSeis data acquisition used receiver spacing of 32.8 ft (10 m) in most locations, with the spacing reduced to 16.4 ft (5 m) in portions of the DCP. The lower range of typical Obispo velocity is 8,000 ft/s below the weathering region in the Phase 1 area. Consequently, the aliasing frequency for 60-degree dips is 70 Hz. The raw SigSeis data with dominant frequencies in the 20 to 50 Hz range are unaliased for all dips for all velocities greater than 6,500 ft (e.g., the region below the shallow soil and upper bedrock weathering zone). The horizontal spatial binning and vertical sampling of the SigSeis data impose a dip resolution limit of 60 degrees or less; dips are aliased and not resolved in the 60 to 90 degree range. The high-pass filtered SigSeis data retain balanced amplitudes in the 20 to 70 Hz frequency band and are thus unaliased for dips of 60 degrees or less. Consequently, inspection of raw SigSeis data ensures that all dips at depths associated with acoustic structures of resolvable dimensions in the data are imaged.

2.3.4.2 Phase 2 Seismic-Reflection Resolution and Depth Extent

The Phase 2 marine terrace 3D volume used consistent 5 m source-receiver spacing, yielding an effective center frequency of 100 Hz in a seismic bandwidth of 20–150 Hz. In the Phase 2 area, shallow soil velocities are typically 2,400 ft/s, thus the depth of a quarter wavelength corresponds to 6 ft. Consequently, in the Phase 2 3D volume the mute extends to only several feet below topography.

For the Phase 2 marine terrace 3D volume, the maximum aperture is about 2,000 ft (610 m) which provides consistent depth imaging to depths of about 820 ft (250 m) in the center of the volume. However, Phase 2 marine terrace 3D volume migration aperture is

	FUGRO CONSULTANTS, INC <i>2012 Onshore Seismic Survey Report</i>	PR No.: PGEQ-PR-21
		Revision: 0
		Page 30 of 81

limited to 180 degrees along the southern and northern sides of the volume; migrations of northeast-dipping deeper reflectors along the northeast margin of the 3D volume and southwest-dipping deeper reflectors along the southwest margin of the 3D volume are incomplete. The final 3D interpretation volume for the Phase 2 marine terrace was reduced to an area within the deployed extent of sources and receivers to reduce edge effects. The very high-resolution (10 × 10 ft horizontal, 2 ft vertical cell dimensions) 3D tomographic arrival-time inversion for the Phase 2 marine terrace provides accurate migration velocities from the ground surface covered in soil, through the buried weathered bedrock zone, to depths of 100 ft below mean sea level. PSDM velocity analyses confirm that reflectors are flat in CIGs using the 3D tomographic velocities for migration.

The seismic-reflection resolution limits of the Phase 2 3D volume are different within the low-velocity soil and the underlying rock, owing to the large velocity differences between the low-velocity soil (2,000–4,000 ft/s) and the high-velocity rocks (10,000–13,000 ft/s). The Phase 2 3D bin sizes of 8 ft (inline) and 16 ft (crossline) set the limits on horizontal data resolution. In the soil section above rock, the typical soil velocity is 3,000 ft/s (ranging from 2,000–4,000 ft/s), and the frequency bandwidth has a 120 Hz center frequency, with a 160 Hz maximum frequency. Consequently, the maximum vertical quarter-wavelength bedding resolution is 5–10 ft, with limits on maximum vertical deflection resolution on the order of 3–5 ft. In rock, there is loss of some frequency bandwidth, so the frequency bandwidth has a 100 Hz center frequency with a 150 Hz maximum frequency. Consequently, in Phase 2 rock, the maximum vertical quarter-wavelength bedding resolution ranges from 15–30 ft, with maximum vertical deflection resolution on the order of 10–20 ft. Minimum horizontal wavelengths of resolvable folding in the soil are on the order of 50 ft, and in rock, on the order of 200 ft.

The aliasing frequency (f_{max}) for a particular receiver group spacing (dx) formation velocity (v) and dip (ϕ) is (Dobrin and Savit, 1988):

$$f_{max} = \frac{v}{4 dx \sin(\phi)} \quad (2-1)$$

For Phase 2 marine terrace data acquisition, the inline receiver spacing was 16.4 ft (5 m) and the crossline receiver spacing was 32.8 ft (10 m). Below the weathering zone, in rock that has velocities of 10,500 ft/s or more, the inline aliasing frequency is 160 Hz and the crossline aliasing frequency is 80 Hz for steep dips. For dips of 45 degrees or less, rock aliasing frequency is 113 Hz in the crossline direction and 226 Hz in the inline direction. Consequently, steep rock dips are resolvable in the inline dip (north-south) direction, but along-strike (east-west), dips are only resolved to dips of 45 degrees. Toward the base of soil, with velocities of 4,000 ft/s, the inline aliasing frequency for dips of 30 degrees is 122 Hz and 61 Hz in the crossline direction; only moderate soil dips are resolvable in soil. The rock weathering zone has an acoustic structure with strong sub-horizontal impedance contrasts that dominate the reflection responses. Dips steeper than 60 degrees

	FUGRO CONSULTANTS, INC <i>2012 Onshore Seismic Survey Report</i>	PR No.: PGEQ-PR-21
		Revision: 0
		Page 31 of 81

in the inline dip direction and 30 degrees in the crossline strike direction are not resolvable within the rock weathering zone in the Phase 2 volume.

2.3.5 Constraints on Seismic Stratigraphy

Seismic-reflection data are most easily interpreted in relatively flat-lying sedimentary strata, rather than complexly folded and faulted sedimentary, volcanic, and metamorphic rocks that characterize the Irish Hills. With these caveats in mind, the seismic reflection data acquired for this study provide valuable new subsurface acoustic imaging data. The strengths and limitations of the seismic stratigraphic constraints these new data are discussed herein.

Typically, borehole velocity and geologic logs are combined with seismic wavelets to provide a seismic signature to correlate seismic-reflection structure with geologic structure. In the 2012 3D study, borehole seismic velocity constraints were available to a maximum depth of about 230 ft (70 m) in the DCPD area (PG&E, 2001). There are no borehole velocity and geologic log constraints deeper than 230 ft (70 m) in the Phase 1 area and no boreholes with velocity and geologic logs in the Phase 2 volume. Thus, there are no deep sonic logs to develop synthetic seismic traces to compare to the 2012 3D seismic-reflection data. Consequently, there is no seismic signature information available for either 3D volume that directly shows the seismic-reflection characteristics of Tertiary Obispo formation, Cretaceous sandstone, or Franciscan basement (the three rock types encountered in this study). Thus, all seismic interpretations of the Phase 1 and Phase 2 3D volumes are based on postulated associations of seismic-reflection characteristics with geologic formations. In this study, the primary information used to associate seismic-reflection packages with geologic formations are surface geologic mapping and acoustic velocity ranges associated with this small subset of formations. Consequently, association of seismic reflectors sequences with particular formations is sometimes ambiguous. The 3D tomography provided a means to correlate some reflectors in the Phase 1 DCPD area with Tertiary diabase intrusives, and to associate velocities with outcropping Cretaceous sandstone and Franciscan basement in the Phase 2 marine terrace area.

2.3.6 Seismic-Reflection Data Image Acoustic Impedance Contrasts

The most important limitation of seismic-reflection data is that seismic-reflection structure does not always correspond to geologic bedding or unconformity structure. Seismic-reflection data show subsurface velocity heterogeneity (acoustic impedance contrasts), and as such are acoustic images. Acoustic reflectors in a seismic-reflection image are not direct images of buried geologic bedding, but if the subsurface geologic conditions juxtapose formations with different velocity structure that creates a resolvable acoustic impedance contrast, the reflection data will show this impedance contrast. The Phase 1 data sets attempt to image very complex geology, including shallow metamorphic and igneous rocks, with substantial logistical limitations imposed on

	FUGRO CONSULTANTS, INC <i>2012 Onshore Seismic Survey Report</i>	PR No.: PGEQ-PR-21
		Revision: 0
		Page 32 of 81

acquisition geometry. This section discusses the imaging potential of the 3D reflection volumes.

In the 2012 3D study area, the most prevalent example of discordance between geologic bedding structure and seismic-reflection structure occurs in the near-surface. Weathering imposes a velocity profile that crosscuts stratigraphic bedding, and the impacts of weathering on acoustic velocity structure sometimes extend up to 150 ft below present-day topography.

In both Phase 1 and Phase 2 seismic-reflection volumes, the processes of uplift along the coast have exposed bedrock to terrestrial weathering. These coastal weathering processes have impacted near surface seismic velocity structure; velocities typically increase by a factor of three over a zone extending from the base of soil to 100–150 ft below topography. This weathering zone is dominated by strong, nearly vertical velocity gradients that produce a zone of strong sub-horizontal reflections between the base of soil and the bottom of the weathering zone. In the Phase 1 and Phase 2 volumes, bedding and/or folding observed in the weathering zone above sea level is often steeply dipping to near vertical (e.g., Figures 2-7 and 2-8), yet shallow reflections are predominantly sub-horizontal. This reflectivity phenomenon is due to the strong changes in acoustic velocity in shallow depths associated with weathering. Shallow acoustic structure in the Phase 2 area weathering zone, imaged as a set of sub-horizontal seismic-reflection marker horizons, tends to have strong lateral continuity.

The coarser and more irregular acquisition geometry in the Phase 1 area generally limits the seismic-reflection interpretation zone to minimum depths of 50–100 ft, and often several hundred feet below the ground surface. Consequently, the influence of weathering is observed only in subsets of Phase 1 data that begin within 50–100 ft of topography.

It is clear that shallow, vertically-dipping strata, like those exposed in the sea cliffs in the Phase 1 area (e.g., Figures 2-7), are too shallow and too small-scale vertically and horizontally to be resolved in the Phase 1 3D seismic-reflection data, because the typical minimum resolvable wavelengths in the SigSeis 3D volume are on the order of 200 ft or more. In other words, these vertically dipping strata exhibit chaotic acoustic reflectivity at the scale of the SigSeis volume. Similarly, in the Phase 2 area, only folded bedding wavelengths longer than 200 ft can be consistently resolved in the 3D volume. For example, vertical bedding (Figure 2-8) in the Cretaceous sandstone exposed at the coast is aliased. The ability of acoustic seismic data to image geologic structure is directly physically related to both the frequency bandwidth of the data and the velocity structure of the underlying rocks.

2.3.7 3D Migration Isotropic Velocity Models

Finally, it is important to note that all the Phase 1 and Phase 2 3D migrations used isotropic 3D velocity models. Isotropic migration of 3D data in areas with nonzero azimuthal velocity anisotropy can produce artificial structure such as small-scale bedding

	FUGRO CONSULTANTS, INC <i>2012 Onshore Seismic Survey Report</i>	PR No.: PGEQ-PR-21
		Revision: 0
		Page 33 of 81

undulations and/or small vertical reflector offsets that can appear as small faults. In a hypothetical scenario, isotropic data artifacts could resemble artificial geologic structure in an area that is actually relatively smoothly dipping and un-faulted. It is common practice in reflection processing to first produce 3D volumes using isotropic velocities for initial interpretation and subsequently refine and update velocities to account for azimuthal anisotropy, if it is found to be significantly nonzero. The interpretations presented in this report correspond to initial interpretations of isotropic velocity migrations of the 3D data. The Phase 2 data acquisition geometry has sufficient azimuth and offset regularity to assess whether anisotropy is significant. The Phase 1 SigSeis and Zland data may contain sufficient information to assess whether anisotropy is significant.



Table 2-1. Summary of Seismic Survey Data

Phase/ Acquisition	Description	Time or Depth	Incline Spacing	Crossline Spacing	Vertical Resolution		Depth Range (ft)
					Bedding Resolution (ft)	Fault Detection Resolution (ft)	
2012 ONSIP Phase 1	Phase 1 high-resolution 3D tomography volume	depth	100	100			surface to 3,000
	Zland 3D reflection volume—beam migrated, agc	depth	30	30	12 to 60	6 to 30	surface to 5,000
	Zland 3D reflection volume—beam migrated, raw	depth	30	30	12 to 60	6 to 30	surface to 5,000
	Zland 3D reflection volume—beam migrated, agc	time	30	30	12 to 60	6 to 30	surface to 5,000
	Zland 3D reflection volume—beam migrated, raw	time	30	30	12 to 60	6 to 30	surface to 5,000
	SigSeis 3D reflection volume—double HP30, raw	depth	30	30	12 to 60	6 to 30	surface to 5,000
	SigSeis 3D reflection volume—agc	depth	30	30	12 to 60	6 to 30	surface to 5,000
	SigSeis 3D reflection volume—raw	depth	30	30	12 to 60	6 to 30	surface to 5,000
	SigSeis 3D reflection volume—agc	time	30	30	12 to 60	6 to 30	surface to 5,000
	SigSeis 3D reflection volume—raw	time	30	30	12 to 60	6 to 30	surface to 5,000
2012 ONSIP Phase 2	High-resolution 3D tomography volume	depth	16	32			surface to 300
	High-resolution 3D reflection volume—filtered	depth	16	8	6 to 30	3 to 15	surface to 200
	High-resolution 3D reflection volume—raw	depth	16	8	6 to 30	3 to 15	surface to 200



Table 2-1. (continued)

Phase/ Acquisition	Description	Time or Depth	Incline Spacing	Crossline Spacing	Vertical Resolution		Depth Range (ft)
					Bedding Resolution (ft)	Fault Detection Resolution (ft)	
2011–2012	11-12 3D tomography volume	depth	200	200			surface to 10,000
	11-12 3D tomography volume—merged velocity and density	depth	200	200			surface to 10,000
	Vibe 3D reflection volume—raw	depth	30	30	650 to 1,300	300-1,000	surface to 4,000
	AWD Line 102—beam migrated, time variant agc	depth	15		15 to 60	10 to 50	surface to 8,000
	AWD Line 102—beam migrated, NO time variant agc	depth	15		15 to 60	10 to 50	surface to 8,000
	AWD Line 102—beam migrated, time variant agc	time	15		15 to 60	10 to 50	surface to 8,000
	AWD Line 102—beam migrated, NO time variant agc	time	15		15 to 60	10 to 50	surface to 8,000
	Vibe 2D arbitrary lines	depth	60 ?		45 to 650	30 to 500	300 to 26,000

	FUGRO CONSULTANTS, INC <i>2012 Onshore Seismic Survey Report</i>	PR No.: PGEQ-PR-21
		Revision: 0
		Page 36 of 81

3.0 GEOLOGIC AND TECTONIC SETTING

An overall goal of the seismic survey project is to build a geologic model that incorporates and honors the geologic data from previous geologic studies, including regional tectonic studies, surficial geologic mapping, and well or borehole stratigraphy. More specifically, the goal of the work is to build a model of the faults and their interrelationships. This section reviews the state of knowledge of the geologic and tectonic setting, beginning with the southwestern Irish Hills region (Section 3.1) and concluding with the Phase 1 and Phase 2 areas (Sections 3.2 and 3.3).

3.1 Irish Hills Geology

The study area (Figure 1-1) extends from Point San Luis to Point Buchon, following the southwestern margin of the Irish Hills. This section reviews the geology of the Irish Hills, including tectonic setting, geologic history, and new gravity and magnetic data that provide constraints on basement architecture.

3.1.1 Tectonic Setting

The Irish Hills lie within the San Luis Bay/Pismo structural block (SLBP), as defined by Lettis et al. (2004; Figure 3-1), which is a topographic high interpreted to be actively uplifting by slip on northwest-trending oblique and pure dip-slip faults (Lettis and Hall, 1994; Lettis et al., 2004). In map view, the faults and intervening blocks define a triangular-shaped structural province called the Los Osos–Santa Maria (LOSM) domain (Figure 3-1). The LOSM domain is deforming through distributed dextral shear as part of the diffuse Pacific–North America transform plate boundary (Lettis et al., 1994, 2004).

At the latitude of the Irish Hills, the Pacific–North America transform plate boundary (i.e., the San Andreas and related fault systems) was initiated in late Oligocene–early Miocene time due to progressive subduction and northwestward migration of the East Pacific Rise against the North America Plate (e.g., Atwater, 1970; Page et al., 1998). The onset of transform faulting was accompanied by the opening of en echelon basins along strike-slip and oblique-slip faults within a transtensional tectonic regime.

The study area lies along the southwestern margin of one of those en echelon basins, the Pismo Basin. Tertiary strata unconformably overlie the pre-Tertiary Great Valley and Franciscan basement over the entire region. Near the coastline in the southern end of the study area, the basin margin is defined in part as the faulted contacts between the Tertiary strata and pre-Tertiary basement rock (described below). The main faults involved here are the Shoreline fault offshore, and onshore along the queried contact of the Olson portion of the San Luis Bay fault, and the San Miguelito fault zone (Figure 1-3). Locally onshore, near the western termination of the San Miguelito fault, the Tertiary basement contact is mapped as an unfaulted unconformity (PG&E, 2014a). Offshore and to the north, the Tertiary strata and basement rocks are juxtaposed along the Shoreline fault zone (Figure 1-3). In the offshore areas south and west of the Shoreline fault, the Tertiary

	FUGRO CONSULTANTS, INC <i>2012 Onshore Seismic Survey Report</i>	PR No.: PGEQ-PR-21
		Revision: 0
		Page 37 of 81

strata unconformably overlie the Cretaceous sandstone and Franciscan basement over the entire region.

3.1.2 Geologic History

Basement rock within the footwall of the San Miguelito–Shoreline fault system consists of the Jurassic–Cretaceous Franciscan Complex (e.g., mélangé, graywacke, and serpentinite), the associated Coast Range ophiolite, and Cretaceous sandstone (Hall, 1973; PG&E, 2014a). To the northeast, Tertiary rocks in the hanging wall of the San Miguelito–Shoreline fault system include marine and volcanoclastic strata and intrusive diabase. From oldest to youngest, the Tertiary strata are the Vaqueros, Rincon, Obispo, Monterey, and Pismo Formations (Figure 1-3). Contrary to the overall map pattern, the thicknesses of the Tertiary strata likely increase in the subsurface to the northeast by reason of syntectonic slip on a buried normal/normal-oblique fault system (PG&E, 2014b).

Beginning in the early Pliocene (~5.3 million years ago [Ma]), the relative Pacific–North America Plate motion changed from transtensional to transpressional (e.g., Page et al., 1998; Lettis et al., 2004). In the Irish Hills, transpressional deformation drove the inversion of the Pismo Basin, which in turn produced the large-scale northwest-trending Pismo syncline, more accurately described as a synclinorium, because of the presence of second- and third-order folding mapped within the overall synclinal closure. This episode of compressional deformation likely created the basement-involved folds that are mapped along the San Miguelito fault, San Luis Bay fault, Shoreline fault, and folds that continue offshore south of the shoreline that are evidenced by seafloor geologic mapping (PG&E, 2014a). For example, the nearshore-offshore stratigraphic relationships south of Olson Hill exhibit outcrop patterns consistent with anticline-syncline pairs continuing south from the southern limb of the Pismo syncline, across the Shoreline fault, towards the Hosgri fault. These map-scale stratigraphic relationships, from north to south, are as follows: Cretaceous sandstone, Jurassic–Cretaceous Franciscan, Cretaceous sandstone, Tertiary Obispo Formation, Cretaceous sandstone, Jurassic–Cretaceous Franciscan, Cretaceous sandstone, Tertiary Obispo Formation, consistent with anticline, syncline, anticline, syncline, respectively. The Shoreline fault is located approximately along the axial trace of the northernmost of these aforementioned anticlinal folds.

An angular unconformity separates the top of the Obispo Formation and the base of Monterey Formation (PG&E, 2014a). The stratigraphic column published in the *Report on the Analysis of the Shoreline Fault Zone, Central Coastal California* (the “Shoreline Report”; Fig. B-4-2 of PG&E, 2011) lists the age of the Obispo Formation as 15.5–15.3 Ma, but this is probably an incomplete age range. The Geologic Mapping Project (GMP) report states that “[r]adiometric dates obtained from tuffs in the lower part of the Obispo Formation range from approximately 18 to 15 Ma [Cole and Stanley, 1998].” No published age constraints for the upper Obispo Formation could be located. The Shoreline Report also describes the unconformity between the Obispo and Monterey as

	FUGRO CONSULTANTS, INC <i>2012 Onshore Seismic Survey Report</i>	PR No.: PGEQ-PR-21
		Revision: 0
		Page 38 of 81

“progressive,” and mentions that along the coastline south of Point Buchon, the contact is gradual and “progresses from interbedded fine-grained diatomaceous and tuffaceous sandstone of the Obispo Formation into interbedded chert and sandstone/siltstone.” The Shoreline Report provides the age range for the Monterey Formation as 11.4–10.5 Ma (PG&E, 2011). The upward-truncated diabase intrusive in the Obispo-Monterey contact northeast of the DCPD indicates, at least locally in the vicinity of the DCPD, a significant unconformity separates the Obispo and Monterey.

Stereonet plots were generated from the updated GMP Plate 1 GIS file attributes using all strike and dip measurements for exposures along the southern limb of the Pismo syncline (Figure 3-2; PG&E, 2014a). Dips measurements from the south-dipping northern limb of the Pismo syncline are not included in these plots. The “global” attitude, or the regional trend based on Plate 1 surface structural data, of the Obispo Formation exposed along the onshore portion of the south limb of the Pismo syncline is 272/37 degrees strike/dip; Obispo strata generally dips approximately 37 degrees to the northeast on the south limb of the Pismo syncline. The Monterey Formation global attitude is 282/23 degrees strike/dip. On the south limb of the Pismo syncline, the Monterey strata also dip to the northeast, with a 14-degree dip discrepancy, indicating that the Monterey Formation is more shallowly dipping, and that the Obispo Formation was tilted prior to the deposition of Monterey Formation. The overall map-scale angular discordance between the Monterey and Obispo Formations implies that a compressional tectonic event deformed the Obispo and an erosional event incised the upper surface of the Obispo strata prior to the deposition of the Monterey Formation.

Inversion of the basin and development of the synclinorium occurred by reverse/reverse-oblique slip on strands (exposed and buried) of the former transtensional fault system (Lettis and Hall, 1994). Uplift, documented by a suite of uplifted marine terraces and faulted surficial deposits, has been ongoing in the study area since at least the last 500,000 years, to as long as 700,000 years, based on emergent terrace flights preserved from elevations near the modern sea level up to at least 247 m (Hanson et al., 1994). Age-elevation relationships among these terraces yield uniform late Quaternary uplift rates of the SLBP of 0.1 and 0.2 millimeters per year (mm/yr; Hanson et al., 1994; Lettis and Hall, 1994). Further, despite differences in elevation between time-correlated terraces, the terraces themselves remain horizontal, indicating that the style of late Quaternary deformation of the western Irish Hills is characterized by rigid block uplift with little or no rotation. This contrasts with the character of the earlier contraction (the compressional folding that created the Pismo syncline and associated folds that extend offshore), which involved large-scale, flexural-slip folding (Lettis and Hall, 1994) and the variable dips of the Tertiary strata. Changes in the uplift rate, on the order of tenths of millimeters per year, are documented along the coastal terraces by discrete steps in shoreline-angle elevations of the Stage 5a and 5e marine terraces (Hanson et al., 1994; Lettis and Hall, 1994). The offsets occur where the terraces cross the so-called Rattlesnake fault and Olson Hill deformation zone (Figure 1-3), both considered here to be subzones of the San Luis Bay fault zone.

	FUGRO CONSULTANTS, INC <i>2012 Onshore Seismic Survey Report</i>	PR No.: PGEQ-PR-21
		Revision: 0
		Page 39 of 81

The San Luis Bay fault zone, in turn, is part of a broader group of onshore and offshore Quaternary-active structures called the Southwestern Boundary zone (e.g., PG&E, 2011). The Southwestern Boundary zone is 4–10 km wide and over 60 km long (PG&E, 2011) and separates the SLBP from the subsiding Santa Maria Valley block to the southwest (Figure 3-1). In contrast to the northwest-trending structural grain of the Irish Hills, the structural grain of the Southwestern Boundary zone is predominantly west to slightly northwest. Geologic relationships across individual structures and focal mechanism solutions of historical earthquakes demonstrate that deformation within the Southwestern Boundary zone is complex and occurs through reverse, strike-slip, and oblique-slip motions (PG&E, 2011; Hardebeck, 2010).

3.1.3 Irish Hills Gravity and Magnetic Structure

The updated Complete Bouguer Gravity Anomaly Map, shown on Figure 3-3, provides the most up-to-date and well-constrained gravity map available, using existing gravity data measurements (PG&E, 2011) and new gravity data (Langenheim, 2014) collected by the U.S. Geological Survey (USGS) to improve gravity constraints along the ONSIP seismic profile alignments and around the DCPD vicinity.

One of the most prominent features on Figure 3-3 delineates a strong gravity gradient extending northwest-southeast along an azimuth of approximately 300 degrees approximately 2 km north of the DCPD. North of the gradient, a trough-like gravity low extends through the axial trace of the Pismo syncline, with Bouguer anomaly values ranging from –9.191 to –17.312 milligals characterizing the low-gravity trough. Within the gravity trough in the axial trace of the Pismo syncline, the Honolulu-Tidewater well (the deepest well in the Pismo syncline), reports Tertiary Obispo Formation rocks at depths up to 9,146 ft below sea level. Unfortunately, the Honolulu-Tidewater well was not drilled deep enough to encounter basement rocks (PG&E, 2014a; PG&E, 2014b). Franciscan basement rocks are exposed at the surface approximately 12,700 ft south of the Honolulu-Tidewater well, and approximately 5,200 ft to the north, corresponding to high gravity values on Figure 3-3.

Outside of the low-gravity trough, relatively high gravity levels are consistent with the presence of shallow high-gravity Franciscan basement rocks, although basement is obscured in this area by younger Tertiary strata of the Pismo syncline exposed at the surface. The higher gravity values south of this gradient are consistent with values observed with Franciscan rocks exposed at the surface in the northern Irish Hills and along the coast from Olson Hill to Point San Luis.

In the southern Irish Hills region, two types of magnetic rocks are present: Franciscan basement and Tertiary Obispo Formation diabase volcanic intrusives. Potential field gravity and magnetic data indicate that relatively high-velocity, high-gravity magnetic rocks are present in the shallow subsurface up to approximately 2 km north of the DCPD (Figures 3-3 and 3-4). The northwest-southeast-trending gravity gradient (300°), approximately 2 km north of the plant, corresponds to the location of shallow magnetic

	FUGRO CONSULTANTS, INC <i>2012 Onshore Seismic Survey Report</i>	PR No.: PGEQ-PR-21
		Revision: 0
		Page 40 of 81

highs imaged in the total magnetic intensity anomaly (helicopter) map shown on Figure 3-4. This gravity and magnetic gradient likely corresponds to a Franciscan basement high that represents the buried southern shoulder of the ancestral Pismo Basin transtensional rift.

3.2 Phase 1 Geology

The surface geology in the Phase 1 area consists of Tertiary Obispo Formation volcanoclastic strata, and later-stage Obispo Formation diabase volcanic intruded into the volcanoclastics. The Obispo Formation strata exhibit varying levels of folding and deformation, with steep to vertically dipping strata exposed along the coast, and more gently north-dipping beds exposed at Green Peak to the northeast. Cretaceous sandstone and Franciscan basement rocks are exposed in the seafloor approximately 500 m south of the coastline, and onshore several km to the east in the vicinity of Olson Hill.

3.2.1 Phase 1 Geologic Mapping at the DCP

Detailed surface geology of the Phase 1 area is shown on Figures 3-5 and 3-6 (PG&E, 2014a, Plate 2). In particular, this map shows the distribution of surface bedrock units, Quaternary geomorphic deposits, and structural measurements (i.e., strike and dip), as well as the locations of known faults and folds. The geologic base map was developed under PG&E's Geologic Mapping Program (PG&E, 2014a). Because this area underlies the facilities of the DCP, geologic mapping was performed in greater detail than the strip mapping effort that took place concurrently throughout the rest of the Irish Hills along select 2011 ONSIP reflection profiles. Note that the map shown on Figure 3-5 includes greater geologic detail relative to the map on Figure 1-3; the Obispo Formation is subdivided into four map-scale sub-units (discussed below), and a greater density of structural measurements is shown.

3.2.2 Phase 1 Stratigraphy

Surface-outcropping bedrock in the Phase 1 area consists exclusively of the Miocene Obispo Formation. In the vicinity of the DCP, the Obispo Formation likely defines the base of the Tertiary Pismo Basin infill nonconformably overlying Jurassic–Cretaceous Franciscan Complex and potentially Cretaceous sandstone basement rocks at depth. Four map-scale sub-units, or lithofacies, were recognized in the Obispo Formation within the vicinity of the DCP and the adjacent offshore (PG&E, 2014a); they are labeled below as they are on the accompanying geologic map and explanation (Figures 3-5 and 3-6):

- Bedded, tuffaceous fine sandstone and siltstone (Tmofb).
- Bedded, shaley siltstone with tuffaceous fine sandstone interbeds (Tmofc).
- Resistant, bedded to massive tuffaceous rocks, including possible “peperite,” a near-source intrusive tuff (Tmor).
- Diabase, massive to jointed (Tmod).

	FUGRO CONSULTANTS, INC <i>2012 Onshore Seismic Survey Report</i>	PR No.: PGEQ-PR-21
		Revision: 0
		Page 41 of 81

The diabase sub-unit intrudes all the other lithologies, and thus is the youngest.

Within the Phase 1 area, bedrock of the Obispo Formation is unconformably overlain by Quaternary surficial units, as follows:

- Pleistocene marine terrace deposits (Qm)
- Alluvial fan sediments from Diablo Canyon (Qaf)
- Shallow- and deep-seated landslides (Qls)

Engineered fill (af) also underlies portions of the roadways and infrastructure at the DCP. The marine terraces and associated deposits were subdivided into two distinct generations based on elevation and geomorphic expression. These are the Q1 and Q2 terraces, which are 80,000 years old (ka) and 120 ka, respectively (Hanson et al., 1994).

3.2.3 Phase 1 Structure

Surface structural data collected within the Phase 1 study area indicate that the Obispo Formation is oriented 272/37 degrees strike/dip along the southern limb of the Pismo syncline (Figure 3-2). This trend is consistent with the structural setting of the Phase 1 area, which is on the southwest limb of the Pismo synclinorium. The overall north dip of Obispo strata changes locally due to a series of discontinuous anticline-syncline fold pairs (Figure 3-5). The GMP elected not to map outcrop-scale structures, and focused instead on capturing the map-scale structures. The GMP report (PG&E, 2014a) states that

“...data collection was focused on mapping structures relevant to the scale of the geologic maps and not to the finer scales of small outcrops. To that end, small-scale structures such as parasitic folds and faults with little offset were generally excluded from the field structural measurements...”

and, “Within the Pismo basin are numerous second-order (herein defined as map-scale) and third-order (herein defined as outcrop-scale) anticlines and synclines that trend northwest-southeast. The GMP geologists were instructed to take bedding measurements that were representative of larger, map-scale fold limbs, so the attitudes on Plate 1 from the GMP data are intended to represent map-scale, and not outcrop-scale, structures.”

So, the southern limb of the Pismo synclinorium is a more complexly folded structure than would appear at first glance at the Plate 1 GMP map. The two longest mapped fold pairs occur at the plant site and in the northeast corner of the Phase 1 area; their axes extend approximately 5,000 ft. The remaining fold axes are generally on the order of 1,000–2,000 ft in length.

Several east-west trending queried lineaments project onshore towards the Phase 1 study area (Figure 3-5). A set of lineaments is located at the south end of Discharge Cove, and a set of two parallel lineaments are mapped approximately in the middle of Unnamed Cove. Originally identified in bathymetric data, these lineaments were mapped offshore with queried onshore continuations. The Unnamed Cove lineament juxtaposes the

	FUGRO CONSULTANTS, INC <i>2012 Onshore Seismic Survey Report</i>	PR No.: PGEQ-PR-21
		Revision: 0
		Page 42 of 81

bedded, shaley siltstone with tuffaceous fine sandstone interbeds (Tmofc) and tuffaceous fine sandstone and siltstone (Tmofb) subunits of the Obispo Formation. The southern Discharge Cove lineament set is mapped along contacts between the resistant tuff (Tmor) and the bedded, tuffaceous fine sandstone and siltstone (Tmofb) sub-units. Finally, a queried lineament is mapped onshore south of Diablo Creek, with no mapped continuation offshore to the west (PG&E, 2014a).

A closer look at the more detailed geologic map (Figure 3-5) shows that Obispo volcanoclastic strata dip steeply to vertically along Discharge Cove, with locally overturned bedding mapped in the vicinity of the DCP. Stratigraphically up-section, bedding dips shallow significantly in Green Peak ridge directly east of Discharge Cove. This discordant bedding relationship is clearly demonstrated in the photos provided on Figure 3-7.

3.3 Phase 2 Geology

In the Phase 2 area, folded and steeply dipping Cretaceous sandstones and Franciscan Complex rocks were eroded to form wave-cut platforms during late Quaternary sea-level highstands (Hanson et al., 1994). The surfaces of the platforms now form an abrupt angular unconformity with overlying 5–10 m thick Quaternary sediments of the emergent marine terraces. The marine terraces of the Phase 2 area are a portion of the many miles of coastal terraces studied in the 1980s as part of the LTSP (PG&E, 1989a, 1990). The results of these studies, which focused on mapping and correlation of the terraces and assessment of their deformation along Quaternary-active faults, are presented by Hanson et al. (1994) and Lettis et al. (1994).

3.3.1 Phase 2 Geologic Mapping

Geologic mapping of the Phase 2 area is presented on Figure 3-8. This map shows the distribution of surface bedrock units, Quaternary geomorphic deposits, and structural measurements (i.e., strike and dip), as well as the locations of known faults and folds. The geologic base map was developed under PG&E's Geologic Mapping Program (PG&E, 2014a). A map showing LiDAR-based topography, bathymetry, and known faults and folds, also from the GMP (PG&E, 2014a), is presented on Figure 3-9.

3.3.2 Phase 2 Stratigraphy

Three bedrock units crop out within the Phase 2 area (PG&E, 2014a; Figure 3-8):

- Jurassic-Cretaceous Franciscan Complex
- Cretaceous sandstones (Ks)
- Squire Member of the Tertiary Pismo Formation (Tpps).

	FUGRO CONSULTANTS, INC <i>2012 Onshore Seismic Survey Report</i>	PR No.: PGEQ-PR-21
		Revision: 0
		Page 43 of 81

The Franciscan Complex consists locally of four sub-units:

- Undifferentiated rocks (KJf)
- Mélange (KJfm)
- Metavolcanic rocks (KJfmv)
- Serpentinite (KJs, or s)

Within the Phase 2 3D seismic data extent, rocks of the Franciscan Complex are restricted in surface outcrop to the northwest corner, although the Franciscan rocks underlie the Cretaceous sandstone sequence across the Phase 2 extent. Franciscan exposures are adjacently present offshore and in isolated upslope exposures in drainages. Geologic mapping indicates that the contacts between the Franciscan sub-units are faulted. Outcrop patterns and lineament assessments indicate chaotic fracturing on scales of tens to hundreds of meters within each sub-unit. Mapping indicates that the upper Franciscan-Cretaceous boundary is a fault contact. The Cretaceous sandstone is locally composed of well-bedded lithic and arkosic facies, with minor shale interbeds, and is unconformably overlain by the Squire Member of the Pismo Formation. The Squire Member is massive, coarse-grained sandstone and is the youngest member of the upper Pismo Formation. Pliocene in age, it is the youngest bedrock unit and last record of marine deposition in the Irish Hills area (PG&E, 2014a).

Bedrock surfaces in the Phase 2 area are locally modified by two wave-cut platforms dated at 80 ka (Q1) and 120 ka (Q2), as mapped by Hanson et al. (1994). The younger marine terrace surface (Q1) is mapped only in a narrow swath along the cliffs in the northern half of the Phase 2 area and is incised into the older marine terrace surface (Q2) that underlies the majority of the broad, flat coastal platform (Hanson et al., 1994). Quaternary units in the Phase 2 area comprise Pleistocene marine terrace deposits (Qm), colluvium (Qc), alluvium (Qal) and landslide deposits (Qls; Figure 3-10). Colluvium deposits are likely conformable with the underlying marine terrace deposits. Based on a series of shallow geotechnical exploration borings along the terrace deposits, the average combined thickness of colluvium, alluvium, and marine terrace deposits is approximately 54 ft (Table 3-1; PG&E, 1989a, 1990). A photograph taken along the sea cliffs near the Rattlesnake fault shows steeply dipping Cretaceous sandstone truncated and overlain by a layer of rounded gravels and cobbles and a thick deposit of colluvium (Figures 2-8 and 3-9). A bedding-parallel shear zone, which may be associated with the fault, appears to be truncated at the base of the gravel layer.

3.3.3 Phase 2 Structure

Surface structural data within the Phase 2 area show that bedding strikes predominantly to the east-west, with more northerly orientations adjacent to the throughgoing faults. Surface bedding dips along the coastal cliffs are generally inclined steeply to the south, or are overturned and inclined to the north. Bedding dips within the Cretaceous sandstone upslope of the terrace platform range from 25 to 70 degrees and are inclined primarily to

	FUGRO CONSULTANTS, INC <i>2012 Onshore Seismic Survey Report</i>	PR No.: PGEQ-PR-21
		Revision: 0
		Page 44 of 81

the north. Bedding dips within the Pismo Formation upslope of the terrace platform range from 10 to 25 degrees (PG&E, 2014a).

Three main faults are mapped in the Phase 2 area: the Rattlesnake fault, Shoreline fault zone, and San Luis Bay fault zone (Figure 3-9). The onshore Rattlesnake and San Luis Bay faults are both mapped with dashed or queried traces crossing the marine terrace deposits, which show no obvious geomorphic expression of these faults. The marine terrace surfaces have been tilled, plowed, and generally anthropogenically disturbed in this area, so human activity may have obscured subtle features that may have been present. However, the major geomorphic features of the terrace surfaces seem to be intact. The LiDAR-generated topographic map shows the shapes of alluvial fans radiating from major creeks, and colluvial slope deposits shed from the hill fronts (Figure 3-9).

The Rattlesnake fault strikes east-northeast as a splay off of the San Luis Bay fault, extending from the base of the hills across the marine terrace to the coast. From the sea cliff, the fault continues westward offshore toward the Shoreline fault. A slight change in the strike of the near-vertical bedding on either side of the fault is evident in the modern wave-cut platform (Figure 3-9). The Rattlesnake fault is mapped on the basis of borehole data, which suggest a step in the bedrock platform in three lines of boreholes drilled across the fault (Figure 3-11; Lettis et al., 1994). Hanson et al. (1994) conclude that the Rattlesnake fault corresponds to an uplift rate boundary along the emergent marine terraces.

The San Luis Bay fault was first identified in an exposure of the marine platform at Avila Beach on the east side of Point San Luis (Lettis et al., 1994). Here the bedrock platform and overlying marine sediments are clearly displaced by faulting. The fault is drawn from Avila Beach west through a slope break in San Luis Hill, then northwest along the back edge of the marine terrace as far as Olson Hill. (Figures 1-3 and 3-8). From there it bends west to join with the Shoreline fault offshore. Existing mapping indicates that this structure juxtaposes Franciscan Complex rocks with Cretaceous sandstones. In addition to these three identified throughgoing faults, several smaller unnamed faults are mapped within the Phase 2 study area along the juxtapositions of Franciscan rocks with Cretaceous sandstone, and include smaller splays off the southeastern termination of the Shoreline fault.

All three of these faults mapped in the Phase 2 area, the Rattlesnake, the San Luis Bay, and the Shoreline faults, have been suggested to be Quaternary active. Hanson et al. (1994) documented an abrupt change in the elevation of the Q2 terrace (~120 ka) back edge (i.e., the shoreline angle) at the Rattlesnake splay of the San Luis Bay fault. They interpret a change in the post-late Pleistocene uplift rate from 0.09 to 0.14 mm/yr across the fault. The Shoreline fault also demonstrates Quaternary activity and was identified based on a linear trend of seismicity (PG&E, 2011).



Table 3-1. Phase 2 Borehole Data Correlating Top-of-Rock Elevation with P-wave Velocity

Line Number	Borehole Number	Lithology of Bedrock	Top-of-Rock Elevation (ft)*	P-Wave Velocity at Top of Rock (ft/s)**
10	DH-095	Ks	58 + 6	6,134
10	DH-096	Ks	45 ± 2	4,365
10	DH-097	Ks	44 ± 5	3,819
14	DH-098	Ks	45	4,632
14	DH-099	Ks	47	4,503
14	DH-100	Ks	46	3,866
10	DH-181	Ks	45.5	3,793
10	DH-182	Not reported	54	4,631
11	DH-183	Ks	34–36	5,479
11	DH-184	Ks	44	5,316
11	DH-185	Ks	50	5,165
11	DH-186	Ks	60	4,892
11	DH-187	Ks	64.5	5,693
13	DH-188	Ks	79	3,237
13	DH-189	Ks	57	4,027
13	DH-190	Ks	51	4,217
13	DH-191	Ks	47	3,724
13	DH-192	Ks	39	3,734
14	DH-193	Ks	54	4,096
17	DH-194	Ks	38	6,399
17	DH-195	Ks	43	6,951
14	DH-196	Ks	88	3,847
14	DH-197	Ks	50	4,198
12	DH-198	Ks	48	4,593
12	DH-199	Not reported	59	4,192
12	DH-200	Ks	51	3,843
12	DH-201	Ks	42	4,542
12	DH-202	Ks	39	4,844
11	DH-203	Ks	130	5,657
11	DH-204	Ks	81	5,479
15	DH-213	Ks	46	4,935
15	DH-214	Ks	46	5,181
15	DH-215	Ks	42	4,795
15	DH-216	Ks	29	5,301



Table 3-1. (continued)

Line Number	Borehole Number	Lithology of Bedrock	Top-of-Rock Elevation (ft)*	P-Wave Velocity at Top of Rock (ft/s)**
15	DH-217	Ks	45	4,163
16	DH-222	Ks	40	5,122
16	DH-223	Ks	28	4,880
37	DH-255	Ks	55	4,829
37	DH-256	Ks	45	4,502
37	DH-257	Ks	33	4,864
37	DH-258	Not reported	28	5,095
38	DH-259	Ks	42.5	4,899
38	DH-260	Not reported	51	4,763
38	DH-261	Ks	35	5,119
39	DH-262	Ks	114.5	4,069
39	DH-263	Ks	63	5,724
39	DH-264	Not reported	50	6,345
40	DH-265	Ks	28	5,997
40	DH-266	Ks	51	6,416
40	DH-267	Ks	73	6,145
40	DH-268	Ks	59	7,371
41	DH-269	Ks	79	4,293
41	DH-270	Ks	69	4,243
41	DH-271	KJfmv	61	4,620
41	DH-272	Ks	68	4,231
mean			54	4,869
standard deviation			20	882

Notes: Borehole data for Lines 10 through 17 are from PG&E (1989a). Borehole data for Lines 37 through 41 are from PG&E (1990).

* Reported uncertainty of the top-of-rock elevation is ± 2 ft unless otherwise noted.

** P-wave velocities are computed from the Phase 2 3D tomographic model, at the top of rock for each borehole.

	FUGRO CONSULTANTS, INC <i>2012 Onshore Seismic Survey Report</i>	PR No.: PGEQ-PR-21
		Revision: 0
		Page 47 of 81

4.0 ANALYSIS, INTERPRETATION, AND RESULTS

This section presents, analyzes, and interprets the 2012 3D seismic survey data within the Phase 1 and Phase 2 areas. Incorporated into the analyses are other geologic and geophysical data collected or compiled for this investigation:

- Updated GMP surface geologic and structural mapping (PG&E, 2014a).
- Potential field magnetic data (PG&E, 2011).
- Updated gravity data (PG&E, 2011; Langenheim, 2014).
- Newly acquired 3D seismic-reflection and Vp tomography data (FCL, 2013a).

This study uses previous data reports, including the marine terrace borehole data from the LTSP (PG&E, 1989a, 1990) and the Shoreline Report (PG&E, 2011).

4.1 Phase 1 Analysis, Interpretation, and Results

The initial Phase 1 structural and stratigraphic assessment of the 2012 3D seismic-reflection and Vp tomography data volumes focused on mapping first-order seismic acoustic-reflector packages in the seismic-reflection amplitude data. Mapping of the seismic-reflection volume was performed side-by-side with the 3D Vp tomographic volume to develop an understanding of both the reflective and tomographic structure, and the relationships between these data volumes throughout the Phase 1 area. After the initial mapping of the Phase 1 Vp tomographic and seismic-reflection amplitude structure, multiple inline and crossline reflection and tomography profiles were assessed to evaluate the presence or absence of queried, tentatively mapped fault structures along their projected onshore trends in the vicinity of Discharge Cove, Unnamed Cove, and the DCP. During this detailed assessment of the presence or absence of tentatively mapped structures in the vicinity of the DCP, the data volumes were thoroughly assessed for the presence of blind, or previously unidentified, fault structures that may offset reflector packages in the seismic-reflection data, or that may offset distinctive Vp velocity bodies delineated in the tomography volume.

4.1.1 Phase 1 Methods of Analysis

The following existing data sets were evaluated for the Phase 1 DCP study area:

- 2012 high-resolution 3D seismic reflection.
- 2012 high-resolution 3D P-wave tomography.
- The most up-to date surface geologic mapping available (PG&E, 2014a).
- Potential field magnetic and gravity data (PG&E, 2011).
- Updated gravity data (Langenheim, 2014).

The Phase 1 study area lies entirely within Obispo Formation rocks at the surface and lacks any deep (>260 ft) borehole data; thus, there are no direct borehole measurements constraining the thickness of the Obispo Formation and the depth to Cretaceous

	FUGRO CONSULTANTS, INC <i>2012 Onshore Seismic Survey Report</i>	PR No.: PGEQ-PR-21
		Revision: 0
		Page 48 of 81

sandstone and/or Franciscan basement rocks underlying the Phase 1 study area (PG&E, 1989b). The Shoreline Report (PG&E, 2011) published updated potential field magnetic and gravity surveys that provide important constraints on basement architecture in the Phase 1 area vicinity and along the south Irish Hills. The USGS obtained new gravity measurements in 2013 that provide infill and improve spatial resolution along ONSIP seismic alignments. The new gravity values were incorporated with existing gravity data to generate the updated 2014 gravity map provided on Figure 3-3 (Langenheim, 2014). The updated gravity map provides improved gravity constraints relative to the gravity maps published in the Shoreline Report (PG&E, 2011).

Recent efforts by the GMP (PG&E, 2014a) provide a preponderance of new surface strike-and-dip data along the coastline near the DCP in the southwestern portion of the Phase 1 area, and a few new strike-and-dip measurements north of the DCP in the northern and northeastern portions of the Phase 1 study area.

The following sections document first-order observations for each data type and discuss the strengths and limitations of these data. The primary goals of mapping these data volumes are as follows:

- To constrain depth to basement rocks (Franciscan and/or Cretaceous sandstone).
- To identify gravity and magnetic gradients with respect to assessing Pismo Basin–edge geometry and constrain the architecture of buried basement rocks.
- To map structural faults and folds.
- To map seismic-stratigraphic packages observed in the reflection data.

Mapping efforts emphasize honoring structural and stratigraphic constraints provided by the GMP surface mapping (PG&E, 2014a). Queried, tentatively mapped surface traces on GMP maps were investigated where features intersect and project into data volumes. In addition, the new data were investigated for the presence or absence of blind or previously undetected faults or offsets.

4.1.2 Phase 1 Vp 3D Tomography Volume

Phase 1 area 2012 3D seismic data were processed to produce both 3D P-wave (Vp) tomography and 3D seismic-reflection volumes. These high-resolution data derived from the 2012 seismic acquisition were merged with the Irish Hills regional 2011 seismic acquisition, regional tomographic, gravity, and density constraints to produce a 3D tomography model of the Irish Hills. The Phase 1 area has a high density of ray paths from the 2012 3D acquisition, and has strong tomographic coverage. The technical details of the tomographic data processing are provided in the PGEQ-08 report (FCL, 2014a). While the irregular seismic acquisition geometry in the Phase 1 area provides inconsistent 3D subsurface reflection coverage and quality, the combination of 2012 Phase 1 seismic travel-time data with 2011 seismic travel-time data and gravity constraints produces a consistent high-resolution 3D Vp subsurface coverage from the near-surface soils to approximately 8,000 ft below sea level. Further, the 3D Vp tomography was refined to

	FUGRO CONSULTANTS, INC <i>2012 Onshore Seismic Survey Report</i>	PR No.: PGEQ-PR-21
		Revision: 0
		Page 49 of 81

provide the highest resolution in the depth range from the near surface to 1,000 ft below sea level, and thus often has vertical resolution comparable to or exceeding 3D reflection resolution of subsurface velocity discontinuities.

The Phase 1 3D Vp tomography used 5 ft vertical cell bins to 300 ft below sea level, 10 ft vertical cells to 1,000 ft below sea level, and 200 ft vertical cells below 1,000 ft below sea level. The 3D tomographic Vp model provides the highest resolution imaging of near-surface Tertiary Obispo strata and related geologic structures.

To place the Vp structure into geologic context, characteristic Vp values are associated with mapped surface geologic units for the south Irish Hills area in the Phase 1 and Phase 2 areas. These characteristic Vp-geologic values are presented on Figure 4-1. The Tertiary Obispo Formation volcanic diabase intrusives have the highest characteristic Vp in the study area. Diabase bodies are the only geologic unit exhibiting Vp \geq 18,000 ft per sec (ft/s) values exceeding the slower Vp values characteristic of all other formations in the study area, including the basement rocks made up of Franciscan Complex, with values of Vp = 12,800–16,500 ft/s, and Great Valley, with typical Vp values of approximately 10,500–12,000 ft/s.

Vp values characteristic of the Tertiary strata in the Pismo Basin include Obispo volcanoclastics, which typically range from 9,200 to 7,300 ft/s, with the caveat that locally, Obispo volcanoclastics are altered by dolomitization, which can cause the Obispo Vp values to elevate to 12,000 ft/s. The association between the presence of altered dolomitization mineralogy and high Vp is based on geologic borehole data and suspension logging evidence obtained near the independent spent fuel storage installation (ISFSI; PG&E, 2001). In the Monterey and Pismo Formation strata, Vp values typically range from 7,300 to 5,500 ft/s. The slowest weathered rock and soil Vp values range from 3,700 to \leq 2,000 ft/s (Figure 4-1). North of the study area, in the vicinity of the Honolulu-Tidewater well in the deeper trough of the Pismo Basin, these characteristic velocity associations are not applicable, as dolomitization reported in the Honolulu-Tidewater well apparently locally affects the Monterey and Obispo Formations and yields higher Vp values (\geq 16,000 ft/s) not typically characteristic of the formations.

Two Vp tomography vertical display lines are shown on Figure 4-2. Vp tomographic profile Line 1, shown on Figure 4-3, combines three line segments that extend west-northwest along the coast from near Deer Canyon Creek, then northwest through the western portion of Green Peak, and north through Crowbar Canyon. In the southeast, on the right-hand side of the tomography image on Figure 4-3, Franciscan (KJf) and Great Valley basement rocks are in contact with Tertiary Obispo diabase volcanic intrusives (Tmod), although the basement-Tertiary contact is obscured and mapped as queried through the Quaternary landslide (Qls) and marine terrace deposits (Qm). Along the western extent of the San Luis Bay fault in the vicinity of Olson Hill, basement and Tertiary rocks are mapped in queried fault contact because the inferred structure is buried by Quaternary marine terrace deposits. The Vp tomography reveals no detectable offset in Vp structure in the basement rock velocity range (red to orange hues in the Figure 4-3

	FUGRO CONSULTANTS, INC <i>2012 Onshore Seismic Survey Report</i>	PR No.: PGEQ-PR-21
		Revision: 0
		Page 50 of 81

color map), and the Obispo diabase (yellow to white $\geq 16,000$ ft/s) is present and shallowly dipping to the west and north.

Map relations are queried along the Tertiary-basement contact, which is also obscured by the Quaternary marine terrace deposits, so the contact could be either faulted or in an unconformable depositional relationship. In the near-vicinity offshore, geologic mapping derived from textural assessment of bathymetric digital elevation model (DEM) data, including some constraints provided by diver rock sample data, indicates both volcanoclastic and diabase intrusive units of the Tertiary Obispo Formation are in contact with Cretaceous sandstone and Franciscan basement rocks north of the Shoreline fault; this contact is queried and could be either faulted or unconformable depositional. The exact nature of this contact is uncertain, but this study honors the GMP mapping as provided, as these maps represent the best currently available constraints (PG&E, 2014a).

In the central line segment between the line bends 1 and 2 on Figure 4-3, shallow, high-velocity ($>16,000$ ft/s) diabase bodies clearly imaged in the V_p tomography plots are mapped at the surface south and north of Green Peak and underlying the DCPD area.

The Line 2 V_p tomographic profile, shown on Figure 4-4, extends from the harbor barrier between Intake and Discharge Coves to the southwest, just east of the DCPD, crossing from Obispo Formation to Monterey Formation and into Pismo Formation strata to the northeast. Along the southwestern portion of this V_p tomography profile, the previously defined “basal” diabase intrusion is mapped as truncated by the Shoreline fault offshore. Based on the best-fitting plane-geometric solution, the surface orientation of the mapped contact boundary between the Obispo volcanoclastic strata and the basal diabase intrusive, the orientation of this contact dips gently south (approx. $\leq 5^\circ$) from just south of the DCPD to the Shoreline fault. This gently dipping diabase orientation is corroborated by the V_p tomography profile (Figure 4-4). Beneath the DCPD, this diabase body is flat lying, and north of the DCPD, the diabase body dips gently (approx. $\leq 10^\circ$) to the north, as imaged in the tomographic volume.

Overall, a gentle north dip of high-velocity, high-density, high-gravity magnetic rocks is strongly corroborated by the following data:

- Updated gravity map (Figure 3-3).
- 3D density model (Figure 4-5), 3D V_p tomography model (Figures 4-5, 4-6, and 4-7).
- Heli-magnetics (Figures 3-4 and 4-8).

At the DCPD location in the subsurface, the basal diabase underlies the volcanoclastic strata and is present at mean sea level (MSL). To illustrate this, Figures 4-6 and 4-7 show depth slices at 358 ft below MSL, and 3 ft above MSL, respectively. Figures 4-4 and 4-7 show a relatively very high-velocity body $\geq 16,000$ ft/s directly under DCPD at 3 ft above MSL. Figure 4-4 illustrates the flat to gently dipping nature of the basal diabase body, exposed offshore north of the Shoreline fault to nearshore along Intake Cove, where the volcanoclastic strata of the Obispo overlie the diabase. To the north of Intake Cove, this

	FUGRO CONSULTANTS, INC <i>2012 Onshore Seismic Survey Report</i>	PR No.: PGEQ-PR-21
		Revision: 0
		Page 51 of 81

flat-lying to gently north-dipping diabase body extends in the subsurface under and to the north of the DCP.

The upper diabase body that is exposed at the surface exhibits a relatively flat-lying surface expression along the north and south slopes of Diablo Canyon north of the switchyard. Based on the surface mapping, this upper diabase body crosscuts bedding and extends up through the Obispo to the unconformable Obispo-Monterey contact, which is also clearly imaged in the tomographic profiles (Figure 4-4). The surface mapping and Vp tomography data corroborate the mapped locations of the diabase bodies.

An important observation to note is that the surface strike and dip measurements in the volcanoclastic units of the Obispo Formation along Discharge Cove indicate the presence of steeply north-dipping and variably overturned bedding. The shallow, flat-lying diabase intrusive body underlying the Obispo Formation in this location indicates that these steep surface dips do not extend to depth. One possible explanation is that discordant shortening or detachment folding occurred in the softer Obispo volcanoclastic sediments that did not significantly shorten or fold the much stronger high-velocity diabase body. This could be attributed to out-of-syncline shortening.

4.1.3 Phase 1 Potential Field Magnetic and Gravity Data

This section presents the newly available and/or updated magnetic and gravity data and discusses the implications of these data to the understanding of basement architecture in the Phase 1 area.

4.1.3.1 Magnetic Data

The Total Magnetic Intensity Anomaly Helicopter map (herein referred to as “Helimag”) encompasses the aerial extent shown on Figure 4-9. The Helimag data were acquired by a low-flying (50 m altitude) helicopter along the coast and Phase 1 area. The Shoreline Report also contains regional-scale aeromagnetic data that was flown at 305 m elevation that images longer-wavelength magnetic structure; these aeromagnetic data are not presented in this report. The Helimag data focus on shallower, higher-resolution magnetic structure appropriate to the Phase 1 and Phase 2 study scale. The data acquisition and processing approach for the Helimag map, “provides better resolution of shallow magnetic anomalies than the aeromagnetic data” (Appendix D of PG&E, 2011). In the Phase 1 area, only two types of rock are magnetic: Franciscan metavolcanics and the diabase volcanic intrusive sub-unit of the Obispo Formation.

The extent of the large magnetic dipole emitted by the DCP is clearly delineated in the detailed Helimag map on Figure 4-9. Within the extent of the outlined dipole artifact, the underlying magnetic signature of the rocks is completely overprinted and does not accurately reflect underlying magnetic structure. Franciscan metavolcanics and serpentinites exposed at the surface onshore and offshore (PG&E, 2011) display a strong magnetic intensity, typically 47,872 nanoTeslas (nT), and exhibit a characteristic

	FUGRO CONSULTANTS, INC <i>2012 Onshore Seismic Survey Report</i>	PR No.: PGEQ-PR-21
		Revision: 0
		Page 52 of 81

magenta color in the Figure 4-9 color-bar plots. Graywacke sub-units of the Franciscan exposed in the northern Irish Hills do not have a strong magnetic intensity signature, nor do they have a strong gravity signature.

The nearly vertical Shoreline fault zone is locally cored with Franciscan metavolcanics in the offshore vicinity of the DCP (PG&E, 2014a), and is clearly delineated by regional seismicity trends. The Shoreline fault is also clearly delineated in the Helimag data (Figures 4-8 and 4-9). Onshore, where surface mapping is more well constrained (e.g., east of Olson Hill), shallow Franciscan rocks are intermittently exposed along eroded areas and drainages underlying the thin (≤ 500 ft thick) Pliocene Squire Formation (Tpps) along the San Miguelito fault zone. In this area, shallow Franciscan rocks exposed at the surface are also characterized by strong magnetic intensity values, approximately 47,872 nT, with a characteristic magenta color in the Figure 4-9 color bar. The magnetic intensity values are lower ($\sim 47,834$ nT) where the Pliocene Squire Formation (Tpps) overlies the magnetic Franciscan rocks, masking the magnetic signal.

Comparing the magnetic intensity values of diabase bodies and Franciscan rocks at surface exposures (PG&E, 2011; PG&E, 2014a), it is clear that diabase intrusives of the Obispo Formation possess a lower magnetic intensity signature relative to Franciscan rocks. GMP surface mapping delineates flat-lying to shallowly dipping diabase intrusive bodies in the slopes north of the DCP; where exposed at the surface, these diabase bodies exhibit typical magnetic intensity ranging from 47,834 to 47,789 nT, relative to higher typical Franciscan values of 47,872 nT (Figures 4-8 and 4-9). On Figure 4-9, the diabase bodies are characterized by red to yellowish-orange colors in the magnetic intensity color map. Along the mapped upper Obispo/lower Monterey contact, the north margin, or upper surface of the upper diabase body crosscuts Obispo volcanoclastic strata. This upper diabase intrusive has an east-west map orientation in both the GMP surface map and the Helimag map. Surface mapping relationships suggest that the top of the Obispo, including the diabase intrusive, is eroded along an angular unconformity. Above the erosional truncation of this upper diabase body, surface structural measurements indicate that the Monterey Formation exhibits a local 80-degree south dip at the surface, implying discordant folding between the Obispo and Monterey Formations that could be attributed to out-of-syncline detachment folding along the Obispo-Monterey contact.

Southeast of the DCP near Olson Hill, the western portion of the San Luis Bay fault system crosses the emergent marine terraces and splays into the Shoreline fault nearshore. At this location, the San Luis Bay fault zone is mapped as a queried, uncertain fault trace juxtaposing the Franciscan and Cretaceous sandstone basement rocks with Tertiary diabase intrusive bodies and volcanoclastic sub-units of the Obispo Formation (Figure 1-3). At this location, the San Luis Bay fault is mapped as a curving contact, obscured by the emergent marine terrace deposits, and projecting east-northeast toward the San Miguelito fault zone onshore, curving offshore, and trending west-northwest, and splaying into the Shoreline fault zone south of the DCP. Offshore, the Shoreline fault juxtaposes the Obispo Diabase and Franciscan-Cretaceous sandstone basement rocks,

	FUGRO CONSULTANTS, INC <i>2012 Onshore Seismic Survey Report</i>	PR No.: PGEQ-PR-21
		Revision: 0
		Page 53 of 81

similar to the onshore portion near Olson Hill. Along this curving contact between diabase and Franciscan basement, the total magnetic intensity anomaly values are typical of the Franciscan basement rocks throughout the study area (Figure 4-9). Thus, at surface exposures, the Obispo diabase alone has a lower magnetic intensity (47,834–47,789 nT) than magnetic Franciscan, and magnetic Franciscan basement rocks alone (~47,872 nT) have an equivalent magnetic signature of magnetic Franciscan, plus overlying or adjacent magnetic Obispo diabase (~47,872 nT; Figure 4-9).

Surface mapping shows two Obispo diabase intrusive bodies exposed in the vicinity of the DCP. First, the “basal” diabase body exposed south of the DCP is mapped at the base of the Obispo Formation, or at least at the base of the portion of the Obispo Formation exposed at the structural level of the onshore and offshore erosional surface. This basal diabase is the intrusive body exposed along the northern margins of the San Luis Bay fault near Olson Hill and the Shoreline fault zone offshore. The upper diabase intrusive body is exposed north of the DCP structurally and stratigraphically higher in the Obispo section. The upper diabase body is erosionally truncated at the top of the Obispo Formation along the angular unconformity between the top of Obispo Formation and the base of Monterey Formation. Helimag data detect these diabase bodies (Figures 3-5 and 4-9).

The Helimag data (Figure 4-9) indicate the presence of shallow, relatively flat-lying magnetic rocks in the southern limb of the Pismo syncline east of the DCP and north of the San Miguelito fault zone. This magnetic body is delineated on Figure 4-9 south of the dashed line labeled as “Northern extent of higher magnetic intensity anomaly.” Plausible explanations for the shallow, relatively flat-lying magnetic intensity signature are the presence of either shallow Obispo diabase volcanic intrusives or shallow magnetic Franciscan basement rocks—or both (Figure 4-8).

4.1.3.2 Gravity

The updated Complete Bouguer Gravity Anomaly map, shown on Figure 3-3, provides the most up-to-date and well-constrained gravity map to date, using existing gravity data measurements (PG&E, 2011) and new gravity data (Langenheim, 2014) collected by the USGS to improve gravity constraints along the ONSIP seismic profile alignments and around the DCP vicinity. One of the most prominent features on Figure 3-3 is the trough-like gravity low extending northwest-southeast along an azimuth of approximately 300 degrees through the axial trace of the Pismo syncline. Complete Bouguer Gravity Anomaly values range from –9.191 to –17.312 milligals along this low-gravity trough. The Honolulu-Tidewater well, the deepest well in the Pismo syncline, reports Tertiary Obispo Formation rocks at depths up to 9,146 ft below sea level. Unfortunately, the Honolulu-Tidewater well was not drilled deep enough to encounter basement rocks (PG&E, 2014a). Franciscan basement rocks are exposed at the surface approximately 12,700 ft south of the Honolulu-Tidewater well, and approximately 5,200 ft to the north.

	FUGRO CONSULTANTS, INC <i>2012 Onshore Seismic Survey Report</i>	PR No.: PGEQ-PR-21
		Revision: 0
		Page 54 of 81

4.1.4 Phase 1 Isosurfaces

Isovelocity and isodensity surfaces are extracted from the 3D V_p tomography and 3D density models for the Irish Hills. The 12,500 ft/s isovelocity surface shown on Figure 4-5 depicts the 3D variability in subsurface elevations of the uppermost instance of the 12,500 ft/s velocity value throughout the Irish Hills. If the 12,500 ft/s value occurs multiple times below an X-Y point, only the upper, or shallower, value is mapped in the isosurface. The isodensity surface of 2.50 grams per cubic centimeter (g/cm³) is shown on Figure 4-10. Appendix A provides isovelocity and isodensity maps for the Irish Hills.

Isotropic velocity and density relationships are discussed at five locations labeled on Figures 4-5 and 4-11. To the southeast on Point San Luis, at Location 1, Cretaceous sandstone and Franciscan metavolcanic and ophiolitic rocks are mapped at the surface; the isovelocity surface indicates the presence of ≥12,500 ft/s rocks above sea level at this location. From Point San Luis heading northwest along the coastline toward the DCP, the 12,500 ft/s isosurface drops in elevation to the northwest at Location 2 (Figures 4-5 and 4-11), where Cretaceous sandstone and Franciscan basement rocks are in contact at the surface along a queried fault strand just north of the queried thicker-line-weight San Luis Bay fault as mapped on Plate 1 of the GMP report (PG&E, 2014a).

At Location 2, the lowest elevation of the 12,500 ft/s isosurface is directly under the mapped contact between Cretaceous sandstone and Franciscan rocks (KJf), and does not extend across the KJf-Tmod contact just to the northwest. Continuing northwest across the Cretaceous sandstone and Franciscan contact, in the area between Locations 2 and 3, the 12,500 ft/s isovelocity surface drops from approximately 555 ft to approximately 1,180 ft below mean sea level, a 625 ft elevation drop over a distance of approximately 1,500 ft.

At Location 3 on Figures 4-5 and 4-11, the 12,500 ft/s velocity surface comes back up in elevation to less than 530 ft below MSL, which potentially corresponds to the obscured Obispo diabase–Franciscan contact. Location 4 shows the shallow high-velocity structure under the DCP comes up to almost sea level in elevation, and corresponds to the basal Obispo diabase body.

At Location 5, shown on Figures 4-5 and 4-11, just south of the Honolulu-Tidewater well, a prominent near-vertical velocity high extends to the northwest all the way to the coast near Islay Creek. South of this near-vertical velocity high, a lower-velocity trough outlines the Pismo Basin, or the southern core of the Pismo syncline. The relationships described in the isovelocity surface are strongly corroborated by the isodensity data (Figures 4-5 and 4-10). One possible explanation for the northwest-southeast-trending high-velocity boundary south of the Honolulu-Tidewater well is the dolomitization reported in the Obispo and Monterey Formations in the well logs; the tomography indicates that V_p values exceeding 17,000 ft/s are present in the Monterey Formation, anomalously high V_p values for this formation in the study area. This dolomitization reported in the vicinity of the Honolulu-Tidewater well could be attributed to Tertiary

	FUGRO CONSULTANTS, INC <i>2012 Onshore Seismic Survey Report</i>	PR No.: PGEQ-PR-21
		Revision: 0
		Page 55 of 81

fluid migration along the Edna fault system bounding the northern Pismo Basin boundary (e.g., PG&E, 2014b). Similarly, dolomitization has also been reported in the Obispo Formation in the DCPD vicinity and may be related to magnesium-rich hydrothermal alteration associated with the emplacement of the Obispo diabase intrusives, potentially along the Tertiary, buried, ancestral, southern Pismo Basin-bounding faults.

4.1.5 Phase 1 Seismic Reflection

The seismic-reflection data resolution and limitations are discussed in detail in Section 2.3. For interpretation of the Phase 1 SigSeis reflection volume, the best shallow, high-resolution reflection data quality falls proximal to portions of the volume with overlapping source and receiver coverages. Receiver records in portions of the volume lacking nearby shotpoints contain deeper, longer-wavelength signal from offset shotpoints, and provide valuable inline and crossline coverage for the 3D processing. The post-processed depth-migrated SigSeis 3D reflection volume was trimmed to maintain the higher quality data within the highest source-receiver coverage area in the central portion of the Phase 1 acquisition extent. The volume was trimmed to excise the poorly-constrained reflection imaging at the edges of the volume in the areas of poorest source-receiver coverage. A polygon titled “SigSeis 3D Data Boundary,” delineates the portion of the Phase 1 SigSeis 3D volume within which interpretation efforts were focused for this study (Figures 2-1 through 2-4). Again, full technical details of the reflection and tomographic processing are detailed in FCL PR-08 (FCL, 2014a).

4.1.5.1 Extracted Phase 1 SigSeis Seismic-Reflection Data

“Vertical Seismic Displays” (VSDs), or 2D vertical slices extracted from the 3D seismic volume, are the primary seismic-reflection data used for interpretation. VSD profiles extracted from the Phase 1 SigSeis 3D volume followed higher-density regions of source and receiver deployments. VSDs were extracted in predominantly dip and strike orientations to create a lattice of intersecting profiles to track geologic structures along 3D subsurface orientations, where possible. Other VSD sets were extracted close to the DCPD area in evenly-spaced north-south profiles to provide imaging continuity for evaluating structures from the coastline along Unnamed Cove and Discharge Cove inland into the Phase 1 SigSeis data coverage. Seismic data interpreters must recognize regions along the alignment lacking shallow imaging in areas with sourcing gaps along the alignment.

4.1.5.2 Phase 1 Seismic-Reflection Interpretation Criteria

The reflection data depth-migration processing relied on the P-wave tomography to provide initial subsurface velocity constraints. Pre-stack depth-migration velocity analyses were conducted to improve reflection imaging, but relatively little adjustment of the P-wave tomographic velocities was necessary to flatten reflectors in CIGs. Consequently, there is good spatial correspondence between locations of high-velocity

	FUGRO CONSULTANTS, INC <i>2012 Onshore Seismic Survey Report</i>	PR No.: PGEQ-PR-21
		Revision: 0
		Page 56 of 81

diabase in the tomographic volume and strong local reflectors in the 3D seismic-reflection data. For example, the high-Vp central cores of diabase bodies are very clearly imaged in the 3D tomography volume (e.g., Figures 4-3, 4-4, 4-6, and 4-7), but generally, only the margins of the high-velocity diabase bodies, or possibly baked contact-metamorphic zones surrounding the diabase intrusives, are imaged in the seismic-reflection amplitudes.

The contacts between diabase and sedimentary units have the largest velocity contrasts in the entire Phase 1 area, with velocity contrasts of up to a factor of three, between 20,000 ft/s diabase and 6,300 ft/s slower portions of sedimentary Obispo Formation. Consequently, the margins of the diabase are the primary reflectors in the seismic-reflection data, whereas the upper, lower, and lateral extents of the intrusive bodies are much more consistently clearly 3D-imaged in the tomography data relative to the reflection imaging. This is due to the high-velocity contrast between the diabase intrusives and the rest of the volcanoclastic Obispo Formation.

To accurately interpret the 3D reflection data, the 3D tomographic constraints must be honored and understood with respect to the reflection volume. To accomplish this to a first order, tomography data are overlain on the seismic-reflection data to delineate high-velocity diabase bodies and depths to typical velocities associated with basement rock in the study area. Often, bright reflectors in the Obispo volcanoclastics overlie high-Vp diabase bodies imaged in the tomography, and may represent contact-metamorphic baked alteration zones in the volcanoclastic units. For example, dolomitization is reported at the surface in volcanoclastic sub-units proximal to diabase intrusives in the Obispo Formation (FCL, 2014d).

Throughgoing seismic-stratigraphic acoustic packages were mapped to delineate the fundamental acoustic structure present in the Phase 1 area. For example, in the SigSeis volume, one of the more prominent and throughgoing acoustic-reflector relationships is a package of continuously upward-truncating seismic reflectors, which could potentially be indicative of an angular unconformity surface. Surface contour maps of several acoustic seismic-reflector packages were generated to track the elevations of the subsurface features throughout the SigSeis 3D volume, although the data coverage gaps made it impossible to track some seismic-stratigraphic packages throughout the entire volume.

In the absence of borehole data to constrain the rock types, formation-velocity associations, Obispo Formation thickness, or depths to diabase bodies, Franciscan, and Cretaceous sandstone basement rocks, the interpretations of geologic units made herein are designed to parsimoniously honor the gravity, helimagnetic, surface mapping, tomography, and seismic-reflection data volumes. A first-order association of Vp ranges associated with geologic formations exposed along the south coast of the Irish Hills provides a framework for jointly interpreting seismic-reflection amplitudes and seismic velocities. The Vp-geologic associations establish a few unique Vp-geologic associations, and also show that non-unique values overlap. The Obispo diabase bodies are

	FUGRO CONSULTANTS, INC <i>2012 Onshore Seismic Survey Report</i>	PR No.: PGEQ-PR-21
		Revision: 0
		Page 57 of 81

distinguishable by high characteristic velocities, but basement rocks can overlap with altered Obispo volcanoclastic strata (Figure 4-1).

Typically, the top of Franciscan Complex is associated with Vp values approximating 12,500 ft/s, and the top of Cretaceous sandstone Vp is typically 10,500 to 11,000 ft/s, each basement rock unit exhibiting distinctive velocities along the south coast in the 3D tomography. The velocities of sedimentary portions of the Obispo Formation are generally less than 10,000 ft/s. Thicker sections of Obispo diabase are generally at least 16,400 ft/s up to 20,000 ft/s, which is much faster than shallow Franciscan basement. Consequently, to first order, it is reasonable to use these velocity-formation associations in joint interpretation of the 3D tomographic velocities and seismic-reflection data.

Interpretations based on this logical framework provide testable hypotheses that can be evaluated, confirmed, or disproved by borehole geophysical and geologic logging investigations that, in the future, may intersect Obispo and basement rocks. For example, if deeper Obispo strata are more extensively altered by dolomitization than shallow Obispo strata with surface constraints, it could be interpreted as basement-velocity rocks.

4.1.5.3 Phase 1 2D SigSeis Reflection Profiles

This section presents seismic-reflection profiles across portions of the Phase 1 area with source-receiver coverage.

SigSeis Crossline 459, shown on Figure 4-12, is a north-south 2D VSD extracted from the 3D SigSeis volume along an alignment with decent, but varying, source-receiver coverage. Source gaps exist from inline 610 to 635 at the south end of the line toward the coast, and from inline 670 to 720 across Green Peak. A receiver gap also exists from inline 680 to 700 across Green Peak (Figures 4-12 through 4-15). Figure 4-12 depicts two versions of SigSeis 3D Crossline 459, one with a double high-pass filter applied to enhance shallow shorter-wavelength seismic-stratigraphic relationships, and the other, the “rawstack,” or unfiltered, version that enhances longer-wavelength structure with somewhat higher overall signal-to-noise. South is to the left in each of these seismic VSDs.

Figure 4-12 shows a bright south-dipping package of reflectors from 325 to 825 ft depth at the south end of the line extending from inline 610 to 640. The same bright reflectors above 825 ft depth roll over along a subsurface anticlinal fold hinge at inline 640 and dip consistently north to inline 740. This anticline is not mapped at the surface. Other than the south limb of the subsurface anticline at the south end of the line, generally, all reflectors above 1,000 ft depth dip shallowly to the north, and reflectors below 1,000 ft either dip to the south or are flat. Figure 4-16 depicts the SigSeis Crossline 458 panel with horizon interpretations overlain on the VSD. The left “Interpreted” panel depicts a green horizon that separates the upward-truncating reflectors below the anticline at the south end of the line. The right image on Figure 4-16 depicts a retro-deformed seismic

	FUGRO CONSULTANTS, INC <i>2012 Onshore Seismic Survey Report</i>	PR No.: PGEQ-PR-21
		Revision: 0
		Page 58 of 81

panel flattened on the green horizon. This flattening reveals a prominent discordant relationship between the panels of reflectors above and below the green horizon.

PG&E's recent mapping updates provide the best geologic data to place these seismic-stratigraphic relationships into context. First, looking to the offshore mapping (PG&E, 2014a), the Obispo Formation unconformably overlies the Cretaceous sandstone (Figure 1-3) over a widespread area south of the Shoreline fault. The total lateral dextral displacement on the Shoreline fault is not well constrained, but Johnson and Watt (2012) assign a minimum of 1.4 km of dextral strike-slip displacement on the Shoreline fault. Assuming that approximately 1.4 km of dextral offset has taken place, for purposes of palinspastic map restoration pertaining to this theoretical discussion, this is a minor offset at map scale when observing the widespread, ubiquitous, angularly unconformable contact of the Obispo Formation over Cretaceous sandstone offshore. Regionally, the Obispo Formation unconformably overlies the Cretaceous sandstone.

Onshore, approximately 3 km southeast of the DCP, Cretaceous sandstone overlies Franciscan basement rocks from Olson Hill east to Avila Bay. The Cretaceous sandstone is highly deformed and exhibits variable bedding orientations, including steeply dipping, vertical, and overturned bedding (e.g., Figure 2-8) lying in faulted contact over the Franciscan rocks. West of Olson Hill, in the nearshore mapping north of the Shoreline fault, a sliver of Cretaceous sandstone is mapped as underlying the Obispo Formation (Figure 4-8; PG&E, 2014a). This is a key map relationship and it indicates the presence of Cretaceous sandstone underlying the Obispo Formation north of the Shoreline fault in the vicinity of the DCP. Furthermore, the mapped orientation of this contact is relatively flat-lying or shallowly dipping.

Figure 4-13 shows SigSeis Crossline 458 high-pass seismic-reflection data with a V_p tomographic overlay. The overlay clearly images the central portions of the diabase intrusive bodies. Bright reflectors above the diabase intrusive bodies are likely contact-metamorphic zones affecting Obispo volcanoclastic strata immediately surrounding the intrusive bodies. The anticline at the southern end of the line is clearly imaged, as are the upward-truncating reflectors mapped below the green horizon.

Figure 4-14 depicts the same extent of SigSeis Crossline 458 with the rawstack (unfiltered) data. Two buried anticlinal axes are imaged in the rawstack data: the southern fold axis at inline 640 and the northern fold axis at inline 675. Figure 4-15 shows interpreted horizons. The green horizon separates the upward-truncating reflectors below from the Obispo strata above.

If these seismic-acoustic reflectors depict bedding, two buried anticlines imaged on Figure 4-15 appear to be detached along the seismic-stratigraphic unconformity boundary, and reflectors are imbricated in the cores of the folds. In the northern fold, the shorter southern forelimb indicates that this is a south-vergent structure. These structures, which are consistent with older, second-order (parasitic, or out-of-syncline)

	FUGRO CONSULTANTS, INC <i>2012 Onshore Seismic Survey Report</i>	PR No.: PGEQ-PR-21
		Revision: 0
		Page 59 of 81

compressional folds that formed contemporaneously with the Pismo syncline, which are present throughout the Irish Hills.

4.1.5.4 2D SigSeis Reflection Vp Tomography Overlay Profiles

This section presents five uninterpreted SigSeis reflection profiles with Vp tomography overlays along five selected transects exhibiting relatively consistent source-receiver coverage.

Line 1, shown on Figure 4-17, is a dip line extending northeast from Discharge Cove, directly through the DCPD to the north, intersecting Obispo volcanic strata as well as diabase bodies at the surface along the northern half of the line (Figure 4-18). Line 2 is a dip line extending from the northern flank of Green Peak and extending across the switchyard (D-061). These two dip lines are approximately 275 m (~900 ft) apart, and exhibit distinctively different velocity and acoustic structure across a short distance. In Line 1, the diabase intrusive body is tabular, throughgoing along the extent of Line 1, gently north-dipping, and apparently cuts up-section with respect to the acoustic reflectors to the south. The tabular $V_p > 16,000$ ft/s body crosscuts a reflector package at inline 715, but otherwise defines a peak-trough acoustic-impedance reflector boundary. To the east, in Line 2 (Figure 4-17), the tabular high-velocity body is not present, and must pinch out to the east into a narrow branch-line intrusive. This observation is consistent with the surface mapping data, which indicate to the first order that the large, tabular intrusive body originated from the west and intruded to the east, bifurcating into smaller bodies that crosscut bedding in the vicinity of SigSeis Lines 1 and 2. The tomography is imaging the same diabase architecture mapped at the surface.

In these unfiltered SigSeis data (Figure 4-17), shallow, bright throughgoing reflectors approximately 125 ft thick from peak to peak in the depth range of 100 ft above MSL to 500 ft below MSL are overlain by shorter-wavelength folded reflectors. This relationship is better imaged in the high-pass filtered data (Figure 4-16) and implies that discordant shortening may have caused softer, slower, less dense volcanic airfall strata to experience more intense folding along detachment boundaries against stiffer, faster diabase bodies that deformed less during folding or faulting.

Figure 4-19 depicts three profiles: Lines 3, 4, and 5. Line 3 is a dip line located southeast of the DCPD and extending from the coastline to the southern flank of Green Peak. Line 4 is a strike line to the north that crosses Diablo Canyon and the exposed upper diabase. Line 5 is a strike line extending from the DCPD southeast to the shooting range along the southern base of Green Peak. In Line 3, the throughgoing reflector truncation is visible at 725–750 ft below sea level, above which north-dipping reflectors are present.

In Line 4, the northernmost SigSeis strike line, a flat-lying, shallow, high-velocity body ($>17,000$ ft/s) roughly 100 ft thick is imaged from 150 to 250 ft below sea level and follows seismic-acoustic reflector structure to a first order. The continuous, bright seismic reflectors plunge gently to the west-northwest, as does the Obispo strata exposed

	FUGRO CONSULTANTS, INC <i>2012 Onshore Seismic Survey Report</i>	PR No.: PGEQ-PR-21
		Revision: 0
		Page 60 of 81

in the south limb of the Pismo syncline and Green Peak. Again, the seismic data shows subsurface structure consistent with the surface mapping.

Line 5 (Figure 4-19) provides a clear example of the throughgoing angular discordance between seismic reflector packages. At a depth of approximately 1,000 ft below MSL, a bright southeast-dipping package of reflectors truncates upward against a horizontal reflector. This is potentially the Cretaceous sandstone/ Tertiary Obispo Formation angular unconformity that represents a geologic time gap of roughly 47 million years. Alternatively, this could be the Franciscan-Obispo contact, or possibly (but less probable) an intraformational Obispo unconformity. The tomography data do not suggest that this angular reflector correlates to a high-velocity intrusive diabase body.

In addition to discussion of SigSeis reflection profiles and reflection-tomography overlays discussed herein, Section 4.1.5.6 provides a more extensive look at north-south seismic images covering the west side of the DCPD turbine building, extending north of Diablo Creek across the terrace east of Unnamed Cove (Figure 4-20).

4.1.5.5 Phase 1 Seismic Horizon Mapping Framework and Uncertainties

This shallowly dipping discordance in acoustic seismic structure across the green horizon on Figures 4-18 and 4-19 could be explained by several geological scenarios, as mentioned briefly in the previous section. The angular seismic-acoustic reflector discordance mapped along the green horizon (Figures 4-18 and 4-19) may indicate the presence of stratified rocks below the green horizon, which underwent a tectonic folding event that took place before the overlying rocks were deposited, resulting in an angular unconformity or nonconformity. These seismic-stratigraphic reflector orientations could represent several admissible geologic relationships. The most plausible, based on similar geologic relationships across the region, is that the green horizon mapped on Figure 4-19 is the angular unconformity incised into the top of the Cretaceous sandstone, overlain by Tertiary Obispo Formation. It is possible that the purple horizon represents Franciscan basement rocks under the Cretaceous sandstone. The Franciscan metavolcanics and mélangé sub-units mapped in the area are not regularly stratified, but the graywacke sub-unit, if present, could be. However, the Cretaceous sandstone exposed offshore and to the southeast of Olson Hill is stratified, and is in angularly unconformable contact with Tertiary Obispo strata over a wide region across the Shoreline fault offshore. Placing these seismic reflector packages into hypothetical frameworks provides plausible, testable hypothetical scenarios.

4.1.6 Assessment of Mapped Structures near the DCPD

This section focuses on a subset of the overall 3D SigSeis volume north-northwest of and adjacent to the DCPD. Several linear features identified in the bathymetric DEM data are included as queried, tentative structures in the GMP Plate 2 mapping (PG&E, 2014a), and the 2012 Phase 1 seismic-reflection and Vp tomography data are well constrained in this

	FUGRO CONSULTANTS, INC <i>2012 Onshore Seismic Survey Report</i>	PR No.: PGEQ-PR-21
		Revision: 0
		Page 61 of 81

vicinity. Where well resolved in this area, comprehensive reflection and tomographic data examples are provided herein.

The SigSeis reflection volume provides dense coverage in the area north-northwest of the DCPD to evaluate these queried structures. This section references a set of Figures depicting 27 north-south-oriented reflection profiles, spaced 30 ft apart, beginning from the western edge of 3D SigSeis coverage near Unnamed Cove. The series of profiles extends 780 ft to the east through the northwest corner of the DCPD footprint (Figure 4-20).

These 27 2D seismic-reflection profiles, extracted from the 3D SigSeis volume, are also presented with Vp tomography transparency overlays on gray-scale seismic-reflection amplitude data to show the associations between acoustic reflectivity and seismic Vp velocity structure. Combined, the seismic-reflection and Vp tomography Figures illustrate the first-order subsurface structure imaged west and northwest of the DCPD (Figures 4-21 through 4-29).

The discontinuous Vp color scale on Figures 4-21 through 4-29 was designed to separate velocity ranges typically associated with specific geologic units. Gray hues are used to represent soil velocities, dark blue for sedimentary portions of the Obispo Formation, the range from light blue to green for Cretaceous sandstone. Yellow to red hues represent both Franciscan basement and thin branchline Obispo diabase bodies (including the dolomitized volcanoclastic strata and zones surrounding the intrusives altered by contact-metamorphic alteration). Purple hues are reserved for fast, thick trunkline Obispo diabase bodies. The overlap of blue hues between Obispo volcanoclastic strata and Cretaceous sandstone was designed to show that the altered, fast Obispo dolomitized zones have velocities that overlap with Cretaceous sandstone velocities in the Phase 1 area.

The closely spaced 2D reflection profiles and tomographic overlays on Figures 4-21 through 4-29, illustrate the overall Obispo acoustic reflectivity and related Vp structure north and northwest of the DCPD. The second- and third-order folding of reflector packages imaging Obispo strata is locally well resolved in the seismic-reflection amplitude data. The reflection data show the size and scale of these second- and third-order fold structures to extend several hundred feet in the strike direction; these fold wavelengths are consistent with structures observed offshore in the bathymetric data.

The anticlinal axis cored by the Tmofc sub-unit of the Obispo Formation mapped at the seafloor lineament in Unnamed Cove (Figure 4-20) is imaged in the westernmost line set on Figure 4-21, profiles 374–376, when projected approximately 300 ft onshore to the east along strike. North-south-oriented reflection profiles provide imaging of this fold structure, which continues east into profiles 377–379 (Figure 4-22). The tomographic-reflection overlay images show flat-lying, less deformed reflectors near the base of the anticline that coincide with the base of a high-velocity region typically associated with Obispo diabase. Over a strike distance of approximately 200 ft, the anticlinal fold

	FUGRO CONSULTANTS, INC <i>2012 Onshore Seismic Survey Report</i>	PR No.: PGEQ-PR-21
		Revision: 0
		Page 62 of 81

amplitude decreases. The fold wavelength also decreases across profiles 380–382 (Figure 4-23) through profiles 383–385 (Figure 4-24) and 386–388 (Figure 4-25).

Continuing 200 ft further to the east, the reflectors indicate that the anticlinal fold closure does not extend this far to the east. At this point, the reflectors roll over into a monocline with a south-dipping limb, and reflectors to the north are flat-lying in profiles 389–391. Here the higher-velocity diabase thins and dies out in extent to the east in profile 391 (Figure 4-26). The monoclinical hinge persists to the east through profiles 392–394 (Figure 4-27), 395–397 (Figure 4-28), and 398–400 (Figure 4-29).

A queried lineament is mapped just south of Diablo Creek in Discharge Cove. The southern extents of profiles 385–400 (Figures 4-25 through 4-29) provide reflection coverage along this lineament that projects toward the DCPD footprint. A bright, continuous, flat-lying reflector package persists along the southern portion of these lines at approximately 400–600 ft below sea level. The tomography overlays indicate that this reflector package is a high- V_p diabase body that attenuates to the east. Reflectivity in the Obispo strata above this bright diabase body reveals shorter-wavelength folding. No steep or vertical offset of the bright diabase body is observed under the queried lineament mapped near Diablo Creek.

Another queried lineament is mapped through the southern portion of Discharge Cove, extending east-southeast just north of Intake Cove along a mapped contact between Tmofc and Tmor sub-units of the Obispo Formation (Figure 4-18). Overturned and vertical bedding is exposed along the coastline in Discharge Cove in this vicinity (Figure 2-7). On Figure 4-19, Line 3 extends perpendicularly to this queried lineament across an area with strong source-receiver coverage. The Line 3 reflection-tomography overlay shows a bright, shallowly north-dipping reflector package that extends from –325 to –725 ft. The bright reflector package does not appear to be offset in this depth range, but shallower reflectors show short-wavelength, low-amplitude folding from –250 to 0 ft.

In summary, the fold structures imaged in the Phase 1 reflection volume formed during the major compressional folding event that formed the Pismo syncline, and these now-dormant fold structures are crosscut by younger, undeformed, datable terrace surfaces. The folded reflectors imaged in the Obispo Formation provide a visible datum for the evaluation of fault offset. No evidence of any throughgoing offset of flat or folded reflector packages was observed in the Phase 1 seismic volume. A thorough evaluation of the Phase 1 seismic-reflection data volume did not identify any throughgoing reflector truncations that were previously unmapped. The Phase 1 seismic-reflection and tomography volumes were evaluated to specifically assess queried lineaments mapped in Unnamed Cove, Discharge Cove, and the DCPD vicinity, and no significant reflector offsets were observed that would indicate that these lineaments were faults offsetting reflectors.

	FUGRO CONSULTANTS, INC <i>2012 Onshore Seismic Survey Report</i>	PR No.: PGEQ-PR-21
		Revision: 0
		Page 63 of 81

4.2 Phase 2 Analysis, Interpretation, and Results

Analysis of the Phase 2 area focuses on the three primary objectives defined in the scope of work (Section 1.3.2), as follows:

1. Mapping the seismic stratigraphy with specific emphasis on the top-of-bedrock surface.
2. Imaging the subsurface nature of previously mapped faults and geologic structures that intersect the Phase 2 seismic-reflection volume.
3. If applicable, identifying and characterizing any geologic structures that were not previously mapped.

To address these objectives, high-resolution 3D seismic data collected along the marine terraces south of the DCPD were processed into tomographic and seismic-reflection volumes (Figure 2-5). These processed data were then analyzed and interpreted, along with other relevant geologic and geophysical data.

This section begins by detailing the methods used to view and analyze the data for the identification and delineation of potential subsurface structures, in Section 4.2.1. In Section 4.2.2 the analysis and results of the seismic tomography are presented. The top of the 4,900 ft/s V_p surface is presented as an initial proxy for the buried base of soil / top of rock surface along the marine terraces. In Section 4.2.3, the analysis and results of the seismic reflection amplitude data are presented, including a map of the elevation of the highest strong reflector derived from the seismic amplitude data, which provides an additional geophysical proxy for mapping the buried top of rock. Maps and profiles of lineaments identified in the seismic amplitude volume are also presented and interpreted. Section 4.2.4 presents the mapping of topographic lineaments from LiDAR data, and compares those to the seismic reflection data, and in some cases, lineaments defined by throughgoing seismic amplitude reflector truncations identified in the 3D volume, to better understand their origin. Finally, in Section 4.2.5 the magnetic field data are reviewed.

Section 4.2.6 considers all the data and presents an assessment of the evidence for faulting, or the absence of faulting, of the bedrock marine terrace platform. The assessment includes discussion of the previously identified Rattlesnake fault, and identification of two potential new linear features identified in the seismic-reflection data.

4.2.1 Phase 2 Methods of Analysis

This section details the methods used to view and analyze the Phase 2 seismic survey data for the identification and delineation of subsurface structures.

4.2.1.1 Phase 2 V_p Tomography Methods

The Phase 2 3D V_p high-resolution tomography volume was derived from the Phase 2 2012 acquisition. The 3D tomographic volume used 10 ft horizontal cell dimensions and

	FUGRO CONSULTANTS, INC <i>2012 Onshore Seismic Survey Report</i>	PR No.: PGEQ-PR-21
		Revision: 0
		Page 64 of 81

2 ft vertical cell dimensions and is described in detail in project report PGEQ-PR-08 (FCL, 2014a). The 3D tomographic volumes were output at the positions of the 3D seismic-reflection volume bins (16 ft inline and 32 ft crossline spacing) to allow overlays of Vp with seismic amplitude and/or other attributes with a vertical output resolution of 2 ft (Table 2-1).

4.2.1.2 Phase 2 Seismic-Reflection Data Methods

Photographs of sea-cliff exposures (Figure 2-8) provide important context for understanding the seismic-reflection imaging. In these photos, steeply dipping Cretaceous sandstone strata are overlain by thin Quaternary deposits. As expected, the Phase 2 seismic-reflection data do not resolve the steep bedding dips in the Cretaceous sandstone; rather, they image these rocks as a flat-lying, acoustically bright body. In other words, seismic reflectors are not expected to appear as steeply dipping geologic strata because the shallow acoustic structure in weathered rock is dominated by strong increases in velocity with depth through the weathering zone. For example, structural data (e.g., strike and dip measurements) along the coast in the vicinity of the Rattlesnake fault indicate steeply dipping beds in the Cretaceous sandstone unit (Figure 2-8), but reflectors at shallow depths in the same area appear horizontal in the seismic-reflection data, corresponding to a vertical zone from the base of soil to below sea level where velocities increase from 4,900 ft/s at the top of weathered rock to approximately 11,000 ft/s below the weathering zone (e.g., Figure 4-30).

In the Phase 2 reflection-amplitude data, bright horizontal reflectors are ubiquitous in the +50 to -50 ft elevation range, coincident with a velocity increase from approximately 4,500 ft/s to 11,000 ft/s imaged in the Vp tomography volume. This steep velocity gradient is interpreted to be attributed to the depth of the weathering profile on the upper unconformity surface of the bedrock; the upper, more intensely weathered rock corresponds to the 4,500 ft/s, and the deeper unweathered rock mass at the base of the zone corresponds to 11,000 ft/s Vp values. Hence, the attitude of the reflectors in this depth range is more strongly controlled by the vertical gradient of the Vp field than the orientation of bedding planes. Similarly, reflector discontinuities within the strong Vp gradient might correlate to changes in the thickness of that zone, such as lateral changes in the vertical velocity gradient.

The top-of-bedrock beneath the Quaternary sediments does not consistently appear as a bright reflector that is traceable through the Phase 2 volume. The base of the Quaternary deposits exhibits Vp values ranging from 4,800 to 5,000 ft/s, and the weathered top of Cretaceous sandstone bedrock exhibits similar Vp values (Table 3-1). Intermittently, the strongest reflector through depth in certain locations corresponds to depths of inferred soil-rock contacts based on boring logs. In other locations there is no strong reflector at the depth of the inferred soil-rock contact, and the strongest reflector occurs 20–30 ft deeper. Attempts to use reflectivity, trace envelope, and derivative of trace envelope to map the top of bedrock produced irregular bedrock surface elevations that sometimes

	FUGRO CONSULTANTS, INC <i>2012 Onshore Seismic Survey Report</i>	PR No.: PGEQ-PR-21
		Revision: 0
		Page 65 of 81

tracked close to tomographic isovelocities, and sometimes oscillated over 10–20 ft laterally in areas with more irregular reflectivity. Some of the variability in reflectivity near the base of soil may be associated with the lateral variability and existence of boulder-cobble lag deposits that could contribute to scattering that can reduce specular reflectivity (e.g., Figure 2-8).

Because the Phase 2 acquisition geometry was optimized to image shallow structure, this study restricts seismic data mapping assessment to depths above 800 ft below sea level. The Phase 2 data are best resolved from the ground surface to 800 ft below sea level; 3D acquisition aperture limits imaging to depths of approximately 800 ft or less. Deeper portions of the volume, from 200 to 800 ft, benefit from a relatively large suite of offsets and azimuths contributing to common-depth-point (CDP) fold than data shallower than 200 ft. Higher frequencies, and thus higher resolution, are preserved in the top 200 ft of the volume, but CDP fold is reduced as depth decreases. Overall, there is a good balance of data quality from approximately 15–20 ft below topography to approximately 800 ft throughout the 3D volume used for interpretation; this 3D interpretation volume was trimmed to an area defined by the source-receiver extents to reduce edge effects.

Planar features defined by reflector truncations observed in the seismic-amplitude data, called planar discontinuities, are traced through the volume in vertical seismic-amplitude cross sections. The results of this mapping are displayed on two select seismic-amplitude depth-slice horizons (a depth slice is a horizontal seismic-amplitude section). Figure 4-31 provides a schematic cross section of the Phase 2 depth-slice locations in relation to the subsurface. The 60 ft above-sea-level (+60 ft) slice primarily images Quaternary deposits on the terraces and intersects bedrock in locations along the northern edge of the volume, based on borehole controls (PG&E, 1989a, 1990). The +60 ft depth slice should intersect bedrock at the Q2 terrace riser, if present (Hanson et al., 1994). The 150 ft below-sea-level (–150 ft) depth slice falls entirely within bedrock, either Cretaceous sandstone or Franciscan Complex.

Within the defined data-resolution limits of the Phase 2 reflection volume (Section 2.3), seismic-amplitude lineament-identification criteria were developed to limit subjectivity and uncertainty in the mapping process. Mapping criteria were developed to focus on identifying laterally and vertically continuous planar discontinuities that offset seismic-amplitude reflector packages. These planar discontinuities could then be evaluated as potential faults.

The planar discontinuity mapping criteria are as follows. For the -150 foot depth slice, mapped planar discontinuities were required to offset otherwise continuous amplitude reflectors at least 10 ft vertically (defined as the detection limit for faults in this dataset), persist for at least 200 ft laterally, and be throughgoing to 800 ft depth. By definition, a geologic fault of seismogenic interest must be throughgoing, so these mapping criteria honor this point. To be detectable in the seismic reflection amplitude volume, the fault would have to juxtapose rocks, or rock against soil, in an orientation that would create an acoustic impedance contrast. To be detectable in the Vp tomography volume, the fault

	FUGRO CONSULTANTS, INC <i>2012 Onshore Seismic Survey Report</i>	PR No.: PGEQ-PR-21
		Revision: 0
		Page 66 of 81

would have to juxtapose rocks, or rock against soil, in an orientation that would create a detectable Vp contrast, or in a manner that would cause acoustic scattering, producing strong diffractions appearing as disrupted zones in the migrated reflectivity volume.

Weak and/or chaotic internal reflectivity characterizes basement rocks in the northwestern portion part of the Phase 2 reflection volume underlain by Franciscan metamorphic rocks, which possess little to no persistent internal reflectivity compared with stratified Cretaceous sandstones in the middle and southeastern portions of the Phase 2 area. This characteristically poor reflectivity affects the interpretability of the Phase 2 data volume where Franciscan Complex rocks occur.

Special criteria were developed for the mapping of planar discontinuities in the +60 foot slice, which images primarily Quaternary sediments (Figure 4-31 D-140). In order to determine if any planar discontinuities mapped in the seismic amplitude data are of significance to locating recent or throughgoing faulting, the planar discontinuities must be observed as a throughgoing feature in vertical slice seismic data that extends upwards through the weathering profile velocity gradient. Because the zone of high vertical velocity gradient is characterized by horizontal reflectors where bedding is known to be sub-vertical, it is possible that structural features are also over-printed to some extent and may not be traceable through this region. Attention is paid to planar discontinuities that can be traced from deeper to shallower reflector truncations. Within the limitations of these criteria, some planar discontinuities visible in the two depth slices are not identified as possible geologic structures because they are not throughgoing. Instead these discontinuous seismic reflector truncations could be attributed to the imaging of localized discontinuities caused by bedding, joints, or local fractures.

4.2.1.3 Phase 2 Methods Using Existing Geologic and Geophysical Data

Phase 2 Surface geologic mapping efforts were focused on the Irish Hills and adjacent areas, with specific focus placed on the area directly surrounding the DCPP in the Phase 1 area. In the Phase 2 area, the updated information primarily consists of additional surface bedding structural measurements. The geologic mapping establishes the lithologic and structural framework for the interpretation of the seismic survey data

Topographic lineaments are mapped in and around the Phase 2 area based on a slope shade image derived from a 2 m LiDAR DEM compiled for the GMP (PG&E, 2014). Lineament mapping is based on visual inspection of the slope shade image and focuses on linear features that extend across topography. Common linear features in this area that are not mapped where positively identifiable include roads, bedding surfaces, drainages, and ridge-lines.

Magnetic field data published in the Shoreline report (PG&E, 2011) useful to the Phase 2 study area include the rotated-to-pole first vertical derivative of the magnetic field data

	FUGRO CONSULTANTS, INC <i>2012 Onshore Seismic Survey Report</i>	PR No.: PGEQ-PR-21
		Revision: 0
		Page 67 of 81

collected by helicopter (hereafter referred to as “RTP Helimag”) data. For this area, the RTP Helimag data provide the highest resolution map available of shallow magnetic features.

Data from 55 shallow boreholes, drilled in the late 1980s, fall within the Phase 2 area and constrain the thickness of Quaternary deposits and depth to top of rock (Figures 3-10, 4-32, and Table 3-1). These borehole data were used to calibrate the seismic reflection data. The borehole locations were spatially referenced in X-Y space by georeferencing borehole location maps (PG&E, 1989a, 1990). Reported ground-surface and top-of-rock elevations are tabulated in Table 3-1. Soil boring locations and top-of-rock data were entered into IHS Kingdom interpretation software for comparison to the seismic-reflection and tomographic data. The top-of-rock elevation entered was not the reported elevation tabulated in Table 3-1, but an elevation determined by subtracting the reported depth to bedrock from a ground-surface elevation interpolated from the LiDAR data. Uncertainty in the digitized borehole location of about ± 50 ft results in some additional uncertainty in the elevation of the top of rock beyond the reported ± 2 ft indicated in Table 3-1. We estimate this uncertainty to be less than ± 10 ft. Access to surveyed borehole coordinates may decrease this uncertainty.

4.2.2 Phase 2 Tomography Volume and Horizons

P-wave velocity (V_p) contrasts in the subsurface are caused by changes in the stiffness and density of rock, attributable factors such as lithologic contrasts, weathering, degree of induration, degree of fluid saturation, and the like. For this study, V_p tomographic models are interpreted in conjunction with borehole constraints to map the top-of-bedrock surface. The first-order features observed in the Phase 2 3D V_p tomography volume are persistent low-velocity regions occurring along each of the major drainages, a high-velocity gradient zone from approximately 50 ft above MSL to 50 ft below MSL, a continuous low-velocity zone from approximately 50 to 100 ft below sea level, and a relatively abrupt northward shallowing of high-velocity material to the northwest.

The low-velocity zones, observed along drainages incising the terrace deposits, are apparent in depth slices at 60 ft above and 150 ft below sea level (Figure 4-33), as well as in cross section (Figure 4-34). The drainage locations visible on Figure 2-5, and from northwest to southeast, are an unnamed east-west channel, the Irish Canyon drainage, Pecho Creek, an unnamed drainage east of Pecho Creek, and the Rattlesnake Canyon drainage. For the two largest drainages in the volume, Pecho Creek and Irish Canyon, this low- V_p effect persists to depths approaching 200 ft below sea level.

Throughout the Phase 2 volume, there is a dramatic increase in V_p between +50 and -50 ft relative to sea level. Across this zone, V_p rapidly increases from approximately 4,000 to 10,000–12,500 ft/s over a 100–150 ft depth range, a factor of 2 to 3 increase in V_p . This velocity gradient spans a velocity range commonly associated with dry soil (3,700 ft/s), Cretaceous sandstone (11,000 ft/s), and Franciscan rocks (12,800 ft/s) in the south Irish Hills and along the coast. Directly under this high-velocity gradient, there is a small

	FUGRO CONSULTANTS, INC <i>2012 Onshore Seismic Survey Report</i>	PR No.: PGEQ-PR-21
		Revision: 0
		Page 68 of 81

decrease in the seismic-velocity or low-velocity zone, approximately 50 ft thick, that is present throughout the volume (e.g., between traces 320 to 509, between 0 and –50 ft elevation; Figure 4-34).

Figure 4-34 shows a relatively higher Vp body shallowing in the northern part of the Phase 2 volume. The tomographic slices taken at +60 and –150 ft relative to sea level (Figure 4-33) also show a pronounced high-velocity zone in the northwest corner of the volume coincident with the surface outcropping of Franciscan basement rocks (Figure 4-32) based on surface mapping (PG&E, 2014a). Based on reasonable associations between the Vp tomography volume and surface mapping, the Franciscan Complex in the Irish Hills area has a typical Vp of approximately 12,500 ft/s, and the Cretaceous sandstone is typically 11,000 ft/s. Roughly following these velocities across Figure 4-34, it appears that rocks with Franciscan velocities remain close to the surface in the northern Phase 2 region, and then step down abruptly just northwest of Pecho Creek, and remain below –500 ft throughout the southern part of the volume.

The contact between Cretaceous sandstone and Franciscan assemblage rocks is only visible in outcrop in the northernmost part of the Phase 2 area, but the Franciscan underlies the Cretaceous rocks offshore and to the southeast along Point San Luis. Because the seismic reflectors in the near surface are overprinted by the high vertical velocity gradient zone, the seismic-acoustic character of the contact is not directly discernable in the reflection-amplitude data. However, high Vp values in the region underlying the mapped Franciscan rocks provide an observable characteristic Vp-geologic association that provides a context to approximate the contact between the two units based on Vp structure. Correlations between lithology and characteristic Vp in the Phase 1 area and the region between Port San Luis and Point Buchon suggest that the transition between Cretaceous sandstone and Franciscan Complex rocks occurs at approximately 12,500 ft/s. In the Phase 2 area, the 12,500 ft/s isovelocity horizon approaches the base of the high-velocity gradient zone near the mapped outcrop of Franciscan Complex rocks (Figure 4-34, 3-7). Based on these relations, the 12,500 ft/s isovelocity surface provides a reasonable and approximate representation of the top of Franciscan Complex rocks in the Phase 2 volume.

The sediment-bedrock interface in the 3D area represents the base of the wave-cut platforms of Quaternary marine terraces and provides a robust strain marker to assess Quaternary offsets. As part of an investigation in the late 1980s, 55 soil borings were drilled along 13 transects or “lines” within the Phase 2 study area, as shown on Figure 3-9 (PG&E, 1989a, 1990). These soil borings were drilled to constrain the depth to bedrock and establish the geometry of the wave-cut platform. Taken in the aggregate, the boreholes in the Phase 2 area encountered bedrock at a mean elevation of 53 ft above sea level, with a standard deviation of 19 ft (Table 4-1; Figure 4-32).

The soil boring data provide constraints on the top of bedrock along these transects, but are not closely spaced enough to render an accurate 3D top-of-bedrock surface across the entire Phase 2 study area. The high-resolution Phase 2 3D tomographic model was

	FUGRO CONSULTANTS, INC <i>2012 Onshore Seismic Survey Report</i>	PR No.: PGEQ-PR-21
		Revision: 0
		Page 69 of 81

correlated to the borehole data to create a model of the top of bedrock surface based on the average velocity at the top of rock. Table 3-1 tabulates the relationship between the top of rock in each boring and the Vp at that depth in the model, and computes the average Vp of the top of rock for the borehole dataset.

On average, a Vp of 4,869 ft/s, with standard deviation of 882 ft/s, was found to correlate to the top of bedrock identified in the boreholes (Table 3-1). Thus, the 4,900 ft/s isovelocity surface shown on Figure 4-35 provides a first-order smooth approximation to map the upper bedrock surface. Where the underlying bedrock is the higher Vp Franciscan Complex, as in the northwestern portion of the study area, the velocity at the top of rock is not as well constrained due to a lack of boreholes in this area. The one borehole reported to encounter Franciscan rock has a Vp at the top of rock well within the range computed for the Cretaceous sandstone, so the difference may be minimal (Table 3-1).

Three profiles along borehole transects C-C', D-D', and E-E' (Figures 4-36, 4-37, and 4-38) provide visual comparison between the elevation of Cretaceous sandstone as seen in the boreholes and the 4,900 ft/s isovelocity horizon. The top of Cretaceous sandstone is shown as a line connecting the elevation of the top of rock encountered in each boring. These profiles show a reasonably good correlation between the 4,900 ft/s Vp isovelocity horizon and the top of the Cretaceous sandstone.

Major features imaged in the 4,900 ft/s Vp isovelocity surface (Figure 4-35) include topographic lows over incised channels, including what appears to be multiple buried abandoned channels along Pecho Creek, and a general shoreward dip of the Vp surface. No features on the 4,900 ft/s isovelocity surface indicate the presence of lateral or vertical displacements of the velocity structure that could indicate significant displacement of different rock types against each other along a fault.

Four of the boring transects shown on Figure 3-10, suggest the presence of a buried, down-to-the-south offset of the top of Cretaceous sandstone that defines the mapped trace of the Rattlesnake fault (Figures 4-37 and 4-38). Previous studies state the top of buried marine terraces are vertically separated by 8–16 ft at this location (PG&E, 1990). Additionally, a large, upward deflection of the top of the Cretaceous unit in two of the profiles (Figures 4-36 and 4-37) indicates the likely location of the Q2 marine terrace shoreline angle along the northeast edge of the coastal platform (Hanson et al., 1994).

4.2.3 Phase 2 Seismic Reflection

The 3D seismic reflection volume provides high-resolution subsurface acoustic imaging for the Phase 2 area south of the DCP. Following the discussion of limitations in Section 2.3, the strongest subsurface reflector was the top of rock beneath the Quaternary sediments. This signal overwhelmed most reflections from internal structural features of the underlying rock, making them challenging to interpret. However, the reflection data were very useful for the following two tasks: (1) to map a few prominent planar

	FUGRO CONSULTANTS, INC <i>2012 Onshore Seismic Survey Report</i>	PR No.: PGEQ-PR-21
		Revision: 0
		Page 70 of 81

discontinuities that extend through the volume, and (2) to create a map of the top of rock based on the elevation of the highest strong reflector. The methods, analysis, and results of these two tasks are presented below.

4.2.3.1 Seismic-Reflector Discontinuity Mapping

Seismic-reflector discontinuity mapping was performed on discrete depth slices (Figures 4-39 and 4-40) and profiles (Figures 4-30 and 4-41) to examine the extent and geometry of planes of truncated or offset reflectors, referred to herein as “planar discontinuities.” For the two depth slices (+60 and –150 ft below sea level), both raw reflection amplitude and the dip of maximum similarity attribute (Figures 4-42 and 4-43) are analyzed and interpreted. In addition to potential structural features, the general locations of the Q2 terrace riser are noted.

Franciscan Complex basement rocks crop out in the northwestern portion of the Phase 2 area, and are inferred to shallowly underlie Cretaceous sandstone as far south as Pecho Creek. In this area, lineament mapping is both difficult and potentially misleading because of the chaotic acoustic structure of Franciscan rocks. No throughgoing seismic discontinuity planes were observed in this region.

Seismic reflection discontinuity planes mapped at +60 and –150 ft depth slices group into three discrete populations based on their strike (Figures 4-39, 4-40, 4-42, and 4-43):

- northwest
- east-northeast
- east

The northwest-striking planes are subparallel to the offshore trace of the Shoreline fault and are present in both the +60 and –150 ft depth slices north of the Rattlesnake fault. A reflection profile perpendicular to the two largest discontinuity planes in this group is presented on Figure 4-41. In this seismic-reflection profile, the two discontinuity planes dip nearly vertical and strike subparallel to each other, with the longest plane extending 1,500 ft along strike. It is unclear whether any of the northwest-striking discontinuity planes extend upward into the shallow reflectors that represent the Quaternary deposits; the data do not confirm or preclude the possibility.

An east-northeast striking discontinuity plane in the southeast corner of the volume is approximately coincident with the mapped trace of the Rattlesnake fault. In profile (Figure 4-30), this feature appears to dip 40 degrees north, which is consistent with Lettis et al. (1994; therein called the “San Luis Bay fault”), who based vertical displacement rate estimations on a presumed dip of 40 to 70 degrees to the north. This discontinuity plane can be traced across the reflection volume and may potentially continue to significant depths, but is weakly expressed in the seismic reflection data and does not show up noticeably in tomographic data.

	FUGRO CONSULTANTS, INC <i>2012 Onshore Seismic Survey Report</i>	PR No.: PGEQ-PR-21
		Revision: 0
		Page 71 of 81

To assess the possibility that the reflector discontinuity plane correlated to the Rattlesnake fault may simply be a marine terrace riser, the Q2 terrace riser was mapped, where present, using borehole controls along the terrace north of the mapped Rattlesnake fault (Figure 4-40). Where present in the Phase 2 reflection volume, the feature mapped as the Q2 terrace riser is characterized by a consistent upward-step of reflectors towards the land, generally north, and is not associated with any throughgoing structures in the bedrock beneath. The feature mapped as the Rattlesnake fault does not have the same seismic characteristics as the terrace riser.

The third set of discontinuity planes strikes east, dips sub-vertically, and occurs the south of the mapped trace of the mapped Rattlesnake fault. These planes generally do not appear to disrupt Quaternary units, and extend off the edge of the 3D volume, precluding length determination.

4.2.3.2 Map of the Highest Strong Reflector

The seismic reflection data were also used to create a map of the elevation of the highest strong reflector, or bedrock reflection surface map (Figure 4-44). This map, because of its high resolution, was found to be the most useful proxy for the top of rock. It appears to image reflectors as small as 20 ft across, capturing many of the asperities created by boulder tops and bedrock knobs that commonly sit above wave-cut platforms. Such roughness is a common feature of the modern wave-cut platform seen in the bathymetric data on Figure 4-44, thus these asperity features are expected in the buried platform. By contrast, the map of the top of the 4,900 ft/s P-wave velocity surface presented in the previous section shows a smooth, undulating surface that shows only the major topographic features (Figure 4-35).

The map of the elevation of the first strong reflector was created by estimating the bedrock reflector elevation for each seismic trace using the time derivative of the trace envelope. The portion of the derivative of the trace envelope, shifted upward 5 percent of its maximum amplitude prior to the first zero crossing, was used to search for the elevation of the first strong reflector. The elevation of the maximum of the derivative of the trace envelope was used to define the elevation of the bedrock surface; if this elevation is less than sea level or greater than 140 ft no bedrock elevation is defined for that seismic trace location.

The bedrock reflection surface map reveals three linear features shown as “platform lineaments” on Figure 4-44. The lineaments are thought to be topographic features of the wave-cut platform. Figure 4-45 shows the detailed view of these lineaments on the bedrock reflection surface, both interpreted and uninterpreted. One lineament is coincident with the previously mapped Rattlesnake fault, the other two are previously unrecognized structures. Based on their geomorphic expression and other geophysical and geologic characteristics, these three platform lineaments are discussed as potential faults in Section 4.2.6.

	FUGRO CONSULTANTS, INC <i>2012 Onshore Seismic Survey Report</i>	PR No.: PGEQ-PR-21
		Revision: 0
		Page 72 of 81

4.2.4 Phase 2 Topographic Lineaments

To understand the geologic context of the platform lineaments and discontinuity planes mapped in the seismic data in the Phase 2 area, linear topographic features were delineated on a slope shade map generated from the 2 m resolution LiDAR-derived digital elevation model (DEM). The topographic lineaments are characterized as linear steps, benches, breaks-in-slope, and linear drainages seen in the DEM, and were not field verified. The resulting lineament map is not intended to be exhaustive, nor is any particular origin of the lineaments implied. However, many of the topographic lineaments are thought to be expressions of bedding strike in the steeply dipping Cretaceous sandstone.

Figure 4-46 shows the uninterpreted image of the DEM slope-map rendering, as well as the same image with two sets of lines: topographic lineaments mapped using the DEM, and the traces of seismic reflection discontinuity planes mapped at 150 ft below sea level in the 3D seismic-reflection volume. Based on the desktop assessment of the slopeshade map, three primary sets of topographic lineaments are defined based on trend:

- northwest-southeast
- east-northeast/west-southwest
- east-west

All three topographic lineament sets have straight-line traces, irrespective of topography.

Figure 4-46 shows that the traces of the seismic reflection discontinuity planes have similar primary orientations as topographic lineaments mapped at the surface. Both the topographic lineaments and the strikes of the discontinuity planes are subparallel to the traces of proximal faults previously mapped at the surface including northwest-southeast striking Shoreline and San Luis Bay faults, the east-west portion of the San Luis Bay fault in the vicinity of Olson Hill, and the east-northeast Rattlesnake fault (Figure 3-7). The -150 ft east-northeast-oriented seismic amplitude lineament in the vicinity of the mapped trace of the Rattlesnake fault in southeastern portion of the Phase 2 reflection volume (Figure 4-46) is subparallel to the onshore and offshore topographic lineaments mapped adjacent to the Phase 2 area.

There is general agreement between the orientation and continuity of seismic amplitude lineaments observed in the Phase 2 reflection data, and linear geomorphic features observed and mapped in the DEM slope shade data. The seismic and topographic lineaments both generally align with orientations of mapped faults in the region and of the strike of bedding.

4.2.5 Phase 2 Potential Field Magnetic Data

The first vertical derivative (FVD) of the reduced-to-pole total magnetic field intensity delineates near-surface magnetic bodies. Areas of larger FVD amplitudes can be particularly useful to reveal the presence or absence of faults with significant slip, which

	FUGRO CONSULTANTS, INC <i>2012 Onshore Seismic Survey Report</i>	PR No.: PGEQ-PR-21
		Revision: 0
		Page 73 of 81

have the potential to juxtapose rock types with differing magnetic properties. Within the 2012 seismic data acquisition extent polygon on Figure 4-47, Quaternary sediments and Cretaceous sandstones are non-magnetic, and the Franciscan metavolcanics rocks are magnetic. FVD helicopter magnetic data were assessed for the presence or absence of faults within the Phase 2 area (Figure 4-47). First-order observations for this dataset are the presence of local large FVD magnetic amplitudes north of Pecho Creek where Franciscan rocks are mapped at the surface, and near the mapped trace of the Rattlesnake fault, where only non-magnetic Cretaceous sandstone rocks are mapped at the surface.

The magnetic bodies imaged to the north of Pecho Creek generally correspond to the region of high Vp found in the tomographic volume. This observation is consistent with the presence of shallow Franciscan Complex rocks that deepen just north of Pecho Creek and remain deep throughout the southern portion of the Phase 2 area. The consistent and generally lower magnetic signature to the south of Pecho Creek is consistent with the presence of Cretaceous sandstone mapped at the surface. The change in magnetic signature approximately correlates with platform lineament 3, crossing the marine terrace just north of Pecho Creek.

The local FVD magnetic high on the hanging wall side of the mapped trace of the Rattlesnake fault is not generally aligned along other linear features, but does lie proximal to a more coherent magnetic body trending to the south-southeast toward Point San Luis.

4.2.6 Assessment of Structures in the Phase 2 Area

This section assesses the evidence for active faulting beneath the marine terrace sediments in the Phase 2 area. The Rattlesnake fault, the only previously mapped fault in the Phase 2 area, is evaluated first, followed by an assessment of two lineaments identified in the new seismic data that may represent the traces of previously unrecognized faults.

4.2.6.1 Assessment of the Rattlesnake Fault

The Rattlesnake fault is the only previously mapped fault that crosses the Phase 2 acquisition area. As reviewed in Section 3.2, the fault trace was located based on a 7–16 ft step in the top of rock, down to the south, observed in four lines of boreholes drilled for the LTSP program (Figure 3-11; PG&E, 1989a, 1990). The fault separates similar facies of Cretaceous sandstone with little or no recognizable dip discordance (PG&E, 2014a); therefore, this structure was not expected to create a large impedance contrast in the seismic data. A slight change in bedding strike is noted along the projection of the mapped fault trace across the modern wave-cut platform. There is no exposure of the fault in the sea cliff.

The seismic survey data are consistent with the presence of a fault at the mapped location, though they do not conclusively demonstrate its presence. The bedrock

	FUGRO CONSULTANTS, INC <i>2012 Onshore Seismic Survey Report</i>	PR No.: PGEQ-PR-21
		Revision: 0
		Page 74 of 81

reflection surface, or map of the highest strong reflector, shows a lineament trending east-northeast that approximately coincides with the previously mapped trace of the Rattlesnake fault (platform lineament 1a on Figure 4-45). The lineament consists of a line of elongated high points in the bedrock surface, with a relatively low bedrock surface on either side. The lineament changes strike midpoint, with the eastern segment (lineament 1a) oriented N78°E, and the western segment (lineament 1b) oriented N70°W. A planar discontinuity coincident with lineament 1a was also mapped in the 60 ft elevation seismic reflection slice (Figure 4-40). In profile, the discontinuity appears as a faint line of planar reflector truncations. The plane strikes approximately N80°E and dips to the north (Figure 4-30). This orientation and dip direction is consistent with previous models of the Rattlesnake fault (Lettis et al, 1994). Lineament 1a, therefore, may coincide with the Rattlesnake fault.

The bedrock reflection map (Figure 4-45) does not confirm the previously reported amount and sense of displacement on the Rattlesnake fault, and may indeed conflict. No consistent down-to-the-south step is seen across this lineament in the map of the highest strong reflector, the highest resolution geophysical proxy for the top of the bedrock platform. Instead, the bedrock surface seems to be fairly consistent in overall elevation, with a strong micro-relief on the order of 10–30 ft. The elongated bedrock highs that define the lineament are similar in height to other bedrock highs observed on the rough surface. The lines of boreholes that were interpreted to show a bedrock step across the fault (Figure 3-11) may have encountered the irregular bedrock surface, and by chance hit high points and low points in a pattern that suggested a consistent step. Additional drilling may have revealed the more irregular bedrock surface.

If there is indeed no measureable vertical displacement of the bedrock platform across the lineament, alternative models must be called upon. For example, (1) the fault may pre-date the bedrock platform, (2) the fault may have mainly strike-slip motion, (3) the lineament may be an expression of differential erosion along bedding planes, or (4) the lineament may be an expression of erosion along an older shear zone similar to ones exposed in the sea cliff (Figure 2-8). The strike of the lineament is very similar to the strike of the bedding and of the older shear zones. Direct exposure of the fault plane, bedrock platform, and Quaternary sediments would provide the best evidence with which to evaluate these alternative models.

Immediately northwest of lineament 1a, the average elevation of the bedrock platform beneath the terrace surface rises slightly and then, as it approaches lineament 2 falls back to the elevation range seen near lineament 1a (Figure 4-45). This “rise” consists of higher high points, but similar low points, so may be an area where more resistant bedrock has been left as elevated remnants on the wave-cut platform. The edge of the rise is does not coincide with the exact location of lineament 1a. Nonetheless, this area may be an expression of differing bedrock characteristics on opposite sides of the fault. Lineament 1b follows more closely southern edge of this rise.

	FUGRO CONSULTANTS, INC <i>2012 Onshore Seismic Survey Report</i>	PR No.: PGEQ-PR-21
		Revision: 0
		Page 75 of 81

4.2.6.2 Assessment of Previously Unrecognized Structures

The bedrock platform surface, as modeled by the map of the highest strong reflector, reveals two lineaments that have characteristics suggesting they may represent fault traces. These platform lineaments, labeled, lineaments 2 and 3 on Figure 4-44, are described below.

Lineament 2 consists of a linear groove in the surface of the buried platform, and extends for about 1,800 ft in the area between Pecho Creek and the Rattlesnake fault. Its orientation of N88°W is consistent with the general strike of bedding exposed in the nearby modern platform. No significant vertical displacement is noted on across this lineament. However, lineament 2 is directly in line with the projection of a major strand of the Shoreline fault zone shown to terminate at limit of the bathymetric data extent in the nearshore (Figure 4-44). Its location, length, orientation, and prominent geomorphic expression suggest lineament 2 may represent the onshore extension of this strand of the Shoreline fault beneath the marine terrace.

This lineament is also mapped as a planar discontinuity in the seismic reflection volume, seen as a steeply dipping to vertical plane extending to 800 ft depth, as shown in profile on Figure 4-41, and in plan view on Figure 4-39.

However, the orientation of lineament 2 parallel to the strike of bedding, and its lack of geomorphic expression adjacent to and west of Pecho Creek, suggest that it may simply be an expression of erosion along a bedding plane or an older bedding-parallel shear zone in the Cretaceous sandstone. A third interpretation is that this lineament represents both a fault and a bedding plane, the fault having followed a pre-existing plane of weakness between beds.

Lineament 3, located between Pecho Creek and Irish Canyon, marks a boundary between generally higher elevations of the bedrock platform to the northwest and lower elevations to the southeast (Figures 4-44 and 4-45). The lineament, best described as a rough boundary, is oriented approximately N60°E. No lineament was mapped here in the seismic reflection volume, however, profile line F-F' (Figure 4-34, top) shows a distinct contrast in reflectivity on either side of this lineament, with higher reflectivity southeast of the lineament. The tomographic profile (Figure 4-34, bottom) shows higher velocity basement rock at depth north of lineament 3, consistent with the presence of the relatively higher velocity Franciscan Complex rock. Magnetic data (Figure 4-47) also show a body of more strongly magnetic rock northwest of lineament 3, again consistent with the presence of Franciscan Complex rock in the shallow subsurface.

Lineament 3, therefore, may represent the trace of a reverse or reverse-oblique fault that juxtaposes Franciscan Complex rocks with the Cretaceous sandstone. Fault activity is not clear. This could be older basement structure related to the flexural-slip compressional folding that created the Irish Hills. Further investigation would be required to investigate the presence of this postulated fault, and potentially estimate its age and activity.

	FUGRO CONSULTANTS, INC <i>2012 Onshore Seismic Survey Report</i>	PR No.: PGEQ-PR-21
		Revision: 0
		Page 76 of 81

5.0 SUMMARY AND CONCLUSIONS

The 2012 3D Onshore Seismic Interpretation Project provides new 3D seismic-reflection and Vp tomography data volumes for two study areas: the Phase 1 volume surrounding the DCPD vicinity and the Phase 2 volume that covers the marine terrace from Irish Canyon to south of Rattlesnake Canyon.

The Phase 1 3D tomographic volume provides new constraints on the subsurface orientations and extents of diabase intrusive bodies. Phase 1 3D seismic-reflection data provide new well-constrained subsurface imaging along certain 2D profiles and 3D subsets of the overall Phase 1 3D volume. Reflection data indicate the presence of shallow-dipping reflectivity associated with the Obispo Formation and show a buried angular reflector discordance, which is interpreted to be the angular unconformity surface between Cretaceous basement and Tertiary Obispo Formation strata.

The Phase 1 reflection data reveal folding in buried reflector packages consistent with out-of-syncline parasitic folding that discordantly detached and shortened Obispo volcanoclastic strata off of stiffer, relatively undeformed diabase bodies. This flexural-slip folding event is old and no longer active, and took place during the compressional uplift event that inverted the ancestral Pismo Basin into the deeply eroded Pismo syncline. Despite differences in elevation between time-correlated uplifted terraces, the terraces themselves remain horizontal, indicating that the style of late Quaternary deformation of the western Irish Hills is characterized by rigid block uplift with little or no rotation. This contrasts with the character of the earlier contraction (the compressional folding that created the Pismo syncline and associated folds that extend offshore), which involved large-scale flexural-slip folding and the variable dips of the Tertiary strata.

In the southern Irish Hills region, two types of magnetic rocks are present: Franciscan basement and Tertiary Obispo Formation diabase volcanic intrusives. Potential field gravity and magnetic data, new seismic-reflection data, and new Vp tomographic data indicate that relatively high-velocity, high-gravity magnetic rocks are present in the shallow subsurface up to approximately 2 km north of the DCPD. Updated gravity maps show a northwest-southeast-trending gravity gradient (300°) approximately 2 km north of the plant, with high values to the south and low values to the north. This gravity gradient is interpreted to correspond to the southern shoulder of the deep portion of ancestral Pismo Basin, with basement rocks relatively shallow to the south.

In the 0–1 km data-resolution depth range of the Phase 1 reflection data, no throughgoing steep or vertical reflector truncations were observed that would indicate the presence of a significant steep fault offset. No obvious evidence of steep, active, shallow-faulting crosscuts folded and flat-lying reflectors, or the throughgoing unconformity horizon mapped in the volume. Any throughgoing faulting in the reflective depth range of 0 to 0.3 km would have to follow shallow to flat unconformities.

Queried fault structures that are tentatively mapped offshore in Unnamed Cove and Discharge Cove project onshore into the Phase 1 reflection data coverage. The along-

	FUGRO CONSULTANTS, INC <i>2012 Onshore Seismic Survey Report</i>	PR No.: PGEQ-PR-21
		Revision: 0
		Page 77 of 81

strike projections of these queried structures were evaluated, and no throughgoing reflector truncations could be mapped along these projected alignments. Furthermore, these queried fault structures are underlain by shallow, almost flat-lying high-Vp bodies imaged in the tomography volume, which are interpreted to be throughgoing diabase intrusives with extents corroborated by mapped surface exposures. The tomography volume shows no expression of steep offsets on the high-Vp diabase bodies, and the reflection data show no expression of reflector truncations across the high-amplitude bright reflectors that delineate the diabase bodies.

The updated GMP Plate 2 surface mapping (Figure 3-5) shows steep, generally north-dipping Obispo volcanoclastic strata exposed along Discharge Cove. The tomography indicates that these steeply dipping strata are underlain by a shallowly north-dipping diabase intrusive. Future efforts that would consider the construction of a stratigraphic cross section through the Phase 1 area must be very wary of using only the surface dip data, and should honor the nearly flat-lying subsurface velocity structure as well.

The Phase 2 seismic-reflection data provide new shallow high-resolution imaging along the marine terraces southeast of the DCCP. Due to the strong contrast in velocity at the sediment-bedrock contact, and the steep to vertical bedding in the underlying Cretaceous sandstone, the top of bedrock could not be delineated with precision using standard seismic reflection profiles. Instead, the top of the bedrock platform beneath the marine terrace deposits was imaged by mapping the elevation of the highest strong reflector. This map shows surprising detail, resolving bedrock topographic elements consistent with typical roughness of a marine bedrock platform. Platform lineaments were mapped on this image, and were correlated with planar discontinuities mapped in the seismic reflection volume.

Three platform lineaments were identified that merit evaluation as potential faults. First, a lineament approximately coincident with the Rattlesnake fault consists of a line of elongated bedrock highs underlain by a faint planar north-dipping discontinuity in the seismic reflection volume. No consistent bedrock step is seen across this lineament or the mapped trace of the Rattlesnake fault.

The second lineament consists of a linear groove in the bedrock surface oriented N88°W about 1,800 ft long between Pecho Creek and the Rattlesnake fault. This lineament is underlain by a vertical planar discontinuity in the seismic reflection volume.

The third lineament consists of a rough boundary between relatively lower to the southeast and higher to the northwest portions of the bedrock platform. This lineament, located between Pecho Creek and Irish Canyon, coincides with a major change in the velocity structure at depth, with high-velocity Franciscan Complex rock to the northwest and relatively lower velocity rock to the southeast. Magnetic field data show high magnetic intensity on the northwest side of the lineament, also consistent with the presence of Franciscan Complex rock.

	FUGRO CONSULTANTS, INC <i>2012 Onshore Seismic Survey Report</i>	PR No.: PGEQ-PR-21
		Revision: 0
		Page 78 of 81

6.0 RECOMMENDATIONS

The results and interpretations herein present the most reasonable interpretations and initial conclusions that honor the data constraints available at this time. This effort completes the initial interpretation phase of work, which is a standard approach in seismic-reflection data acquisition, processing, and interpretation. To refine and constrain the initial interpretations provided herein, the industry-standard approach is to obtain targeted subsurface geologic and geophysical controls, which provide constraints and additional information to test the initial interpretations.

Downhole geologic and geophysical logs provide the data to generate synthetic seismograms, which improve understanding on the seismic-reflective nature of each geologic unit and depths to bedrock contacts, and provide detailed information on the velocity-depth structure for future data reprocessing to improve and further constrain imaging. Subsurface investigations would also constrain the depths to significant contacts, such as Obispo basement, type of basement, and detailed bedding dip information to help understand how complex folds open and close, and to understand how apparent unit thicknesses are controlled by existing geologic structures. Last, subsurface controls help mis-tie and spatially adjust depth-migrated seismic-amplitude data to reflect subsurface depth structure as accurately as possible.

Three lineaments mapped on the bedrock surface beneath the marine terrace sediments in the Phase 2 area merit investigation as potential faults. In order to directly examine the potential fault plane, ground-based investigations of the bedrock platform surface and the overlying Quaternary sediments would be required. Recommended investigation methods include detailed mapping of the sea cliff and incised creek banks where each of the lineaments would project, and excavations to expose the platform where the sediments are thin enough for excavations to be feasible.

	FUGRO CONSULTANTS, INC <i>2012 Onshore Seismic Survey Report</i>	PR No.: PGEQ-PR-21
		Revision: 0
		Page 79 of 81

7.0 REFERENCES

- Atwater, T.M., 1970. Implications of plate tectonics for the Cenozoic tectonic evolution of western North America, *Geological Society of America Bulletin* **81**: 3513–3536.
- California Energy Commission (CEC), 2008. AB 1632 Assessment of California's Operating Nuclear Plants, final report prepared by MRW & Associates, Inc., CEC-100-2008-005-F, 315 pp.
- Dobrin, M.B., and Savit, C.H., 1988. *Introduction to Geophysical Prospecting*, Fourth Edition, McGraw-Hill College, 867 pp.
- Fugro Consultants, Inc. (FCL), 2012. PGEQ PR-07, Validation of the Commercial Software IHS Kingdom Version 8.6 Hotfix 4 2d/3dpak, Vupak, and Rock Solid Attributes.
- Fugro Consultants, Inc. (FCL), 2013a. *PGEQ PR-14, CCCSIP Onshore 2012 Data Report, Revision 0*, submitted to Pacific Gas & Electric Company on 8 September 2013.
- Fugro Consultants, Inc. (FCL), 2013b. *PGEQ-PR-17, 2012 PG&E P-Cable Low-Energy Seismic Survey, 3D Data Processing Report, San Luis Bay*.
- Fugro Consultants, Inc. (FCL), 2013c. *PGEQ-PR-18, 2012 PG&E P-Cable Low-Energy Seismic Survey, 3D Data Processing Report, Point Sal*.
- Fugro Consultants, Inc. (FCL), 2013d. *PGEQ-PR-19, 2012 PG&E P-Cable Low-Energy Seismic Survey, 3D Data Processing Report, Estero Bay*.
- Fugro Consultants, Inc. (FCL), 2014a. *PGEQ-PR-08, 2011 and 2012 Data Processing Report*.
- Fugro Consultants, Inc. (FCL), 2014b. *PGEQ-PR-16, DCP P- and S-wave Foundation Velocity Report, Revision 0*.
- Fugro Consultants, Inc. (FCL), 2014c. PGEQ-PR-20, QA Documentation for 2012 ONSIP Data Processing and Interpretation.
- Fugro Consultants, Inc. (FCL), 2014d. Confirmation of Foundation Conditions at the DCP P ISFSI Pads Nos. 3 to 7, Calculation package 2277-CALC-01.
- Hall, C.A., Jr., 1973. Geologic map of the Morro Bay South and Port San Luis quadrangles, San Luis Obispo County, California: U.S. Geological Survey Miscellaneous Field Studies Map MF-511, scale 1:24,000.
- Hanson, K.L., Wesling, J.R., Lettis, W.R., Kelson, K.I., and Metzger, L., 1994. Correlation, ages, and uplift rates of Quaternary marine terraces: South-central coastal California: in Alterman, I.B., McMullen, R.B., Cluff, L.S., and Slemmons, D.B. (editors),

	FUGRO CONSULTANTS, INC <i>2012 Onshore Seismic Survey Report</i>	PR No.: PGEQ-PR-21
		Revision: 0
		Page 80 of 81

Seismotectonics of the Central California Coast Ranges: Boulder, Colorado, Geological Society of America Special Paper 292, pp. 45–71.

Hardebeck, J.L., 2010. Seismotectonics and fault structure of the California central coast: *Bulletin of the Seismological Society of America* **92**: 2264–2276.

Johnson, S.Y., and Watt, J.T., 2012. Influence of fault trend, bends, and convergence on shallow structure and geomorphology of the Hosgri strike-slip fault, offshore central California, *Geosphere* **8** (6): 1632–1656.

Langenheim, V.E., 2014. *Gravity, Aeromagnetic and Rock-Property Data of the Central California Coast Ranges*: U.S. Geological Survey Open-File Report 2013-1282, 12 pp., <http://dx.doi.org/10.3133/ofr20131282>.

Langenheim, V.E., Jachens, R.C., Graymer, R.W., and Wentworth, C.M., 2008. Implications for fault and basin geometry in the central California Coast Ranges from preliminary gravity and magnetic data, *EOS* (Abs. AGU), Fall Meeting 2008, abstract #GP43B-0811.

Lettis, W.R., and Hall, N.T., 1994. Los Osos fault zone, San Luis Obispo County, California: in Alterman, I.B., McMullen, R.B., Cluff, L.S., and Slemmons, D.B. (editors), *Seismotectonics of the Central California Coast Ranges*, Geological Society of America Special Paper 292, pp. 111–132.

Lettis, W.R., Hanson, K.L., Unruh, J.R., McLaren, M., and Savage, W.U., 2004. *Quaternary Tectonic Setting of South-Central Coastal California*: U.S. Geological Survey Bulletin 1995-AA, 24 pp, <http://pubs.usgs.gov/bul/1995/aa>.

Lettis, W.R., Kelson, K.I., Wesling, J.R., Hanson, K.L., Angell, M., and Hall, N.T., 1994. Quaternary deformation of the San Luis Range, San Luis Obispo County, California: in Alterman, I.B., McMullen, R.B., Cluff, L.S., and Slemmons, D.B. (editors), *Seismotectonics of the Central California Coast Ranges*: Boulder, Colorado, Geological Society of America Special Paper 292, pp. 111–132.

Pacific Gas and Electric Company (PG&E), 1989a. Response to Question Q43i, Vol 4: Basic Data Report—Borehole and well data, and Vol. 5: Field logs of PG&E and Pacific Geosciences boreholes, Diablo LTSP 1989 DCL 89-22.

Pacific Gas and Electric Company (PG&E), 1989b. Response to Question 19, asked of PG&E by the U.S. Nuclear Regulatory Commission on 13 December 1988 regarding the Final Report of the Diablo Canyon Long Term Seismic Program.

Pacific Gas and Electric Company (PG&E), 1990. Response to Question GSG 16 asked by the U.S. Nuclear Regulatory Commission on August 1, 1989, regarding the Final Report of the Diablo Canyon Long Term Seismic Program.

	FUGRO CONSULTANTS, INC <i>2012 Onshore Seismic Survey Report</i>	PR No.: PGEQ-PR-21
		Revision: 0
		Page 81 of 81

Pacific Gas and Electric Company (PG&E), 2001. Analysis of bedrock stratigraphy and geologic structure at the DCPD ISFSI Site, Geosciences Calculation Package GEO.DCDD.01.21, Rev. 2, Dec. 14, 2001.

Pacific Gas and Electric Company (PG&E), 2011. *Report on the Analysis of the Shoreline Fault Zone, Central Coastal California*, report to the U.S. Nuclear Regulatory Commission, January;
www.pge.com/myhome/edusafety/systemworks/dcpp/shorelinereport/.

Pacific Gas and Electric Company (PG&E), 2012. *DCDD 3D/2D Seismic-Reflection Investigation of Structures Associated with the Northern Shoreline Seismicity Sublineament of the Point Buchon Region*, PG&E Technical Report GEO.DCDD.TR.12.01, Rev. 0, 68 pp.

Pacific Gas and Electric Company (PG&E), 2014a. *Geologic Mapping and Data Compilation for the Interpretation of Onshore Seismic-Reflection Data*, PG&E Technical Report GEO.DCDD.TR.14.01, Rev. 0, 70 pp., 2 plates, and 5 appendices.

Pacific Gas and Electric Company (PG&E), 2014b. *ONSIP 2011 Data Report*, PG&E Technical Report GEO.DCDD.TR.14.03, Report submitted to the U.S. Nuclear Regulatory Commission, June.

Page, B.M., Thompson, G.A., and Coleman, R.G., 1998. Late Cenozoic tectonics of the central and southern Coast Ranges of California. *Geological Society of America Bulletin* **110**: 846–876.

State of California, 2006. Warren-Alquist State Energy Resources Conservation and Development Act, Assembly Bill No. 1632, amendment to Section 25303 of the Public Resources Code.